University of Cambridge, 3D Ultrasound Research

Sequential 3D Diagnostic Ultrasound using the Stradx System

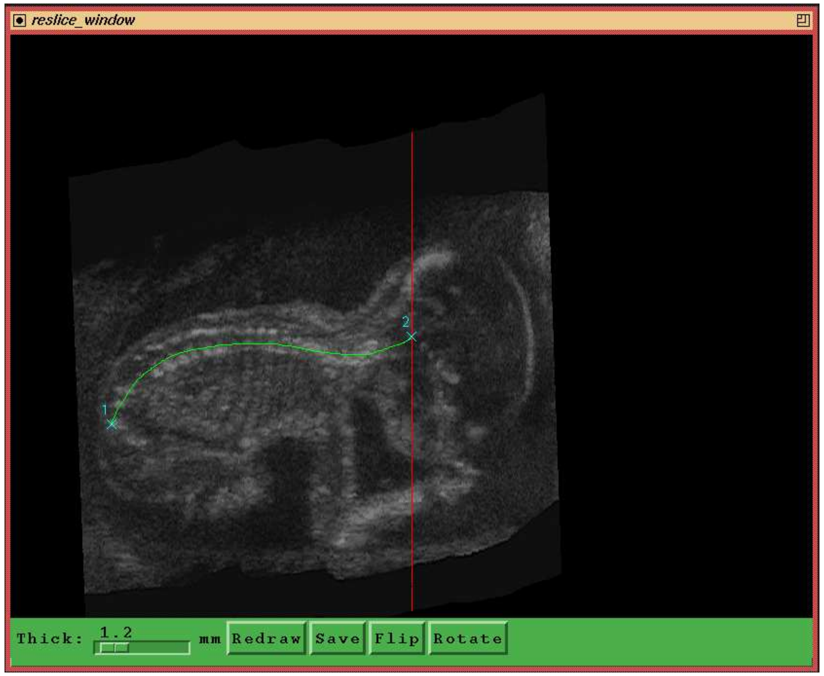

Andrew Gee, Richard Prager & Graham Treece

June 2001

Sequential freehand 3D ultrasound

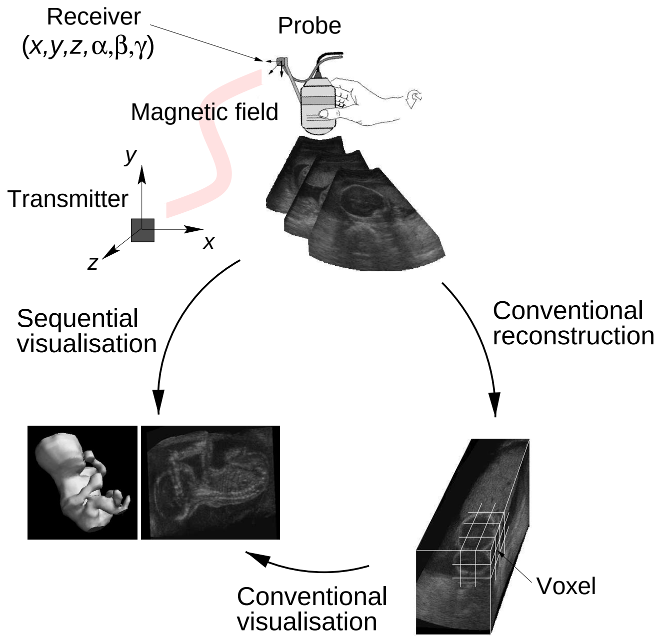

This tutorial will cover:

- Calibration (temporal and spatial).
- Reslicing and volume rendering.
- Panoramic imaging (real time).
- Segmentation and volume estimation.
- Correcting probe pressure artefacts.

Sequential freehand 3D ultrasound

Advantages of a freehand approach:

- Scan unlimited volume of the body.
- Use standard, commercially available ultrasound machines.
- Comparatively cheap.
- Can be accurate.
- Combine scans from different directions.

Advantages of a sequential approach:

- More accurate visualisation (less resampling).
- Lower memory overhead.
- Real-time capabilities.
- More robust segmentation in the original B-scans.

Temporal calibration

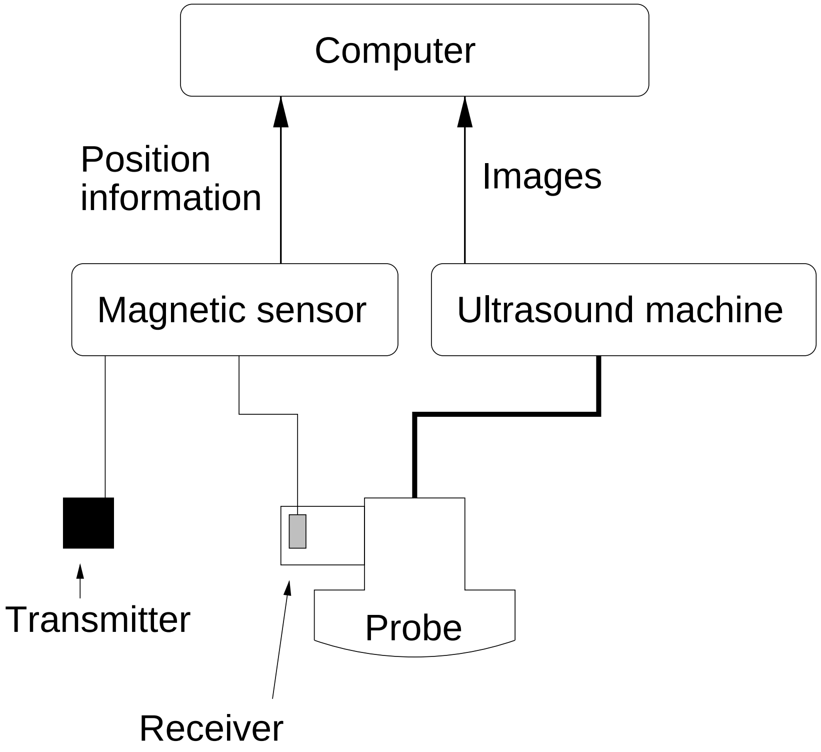

How do we match the positions and images?

The incoming data streams are asynchronous. The image stream runs at 25Hz (PAL), while the position stream runs at 30Hz.

Temporal calibration

The images and positions are time-stamped when they are received by the computer and then stored in circular buffers.

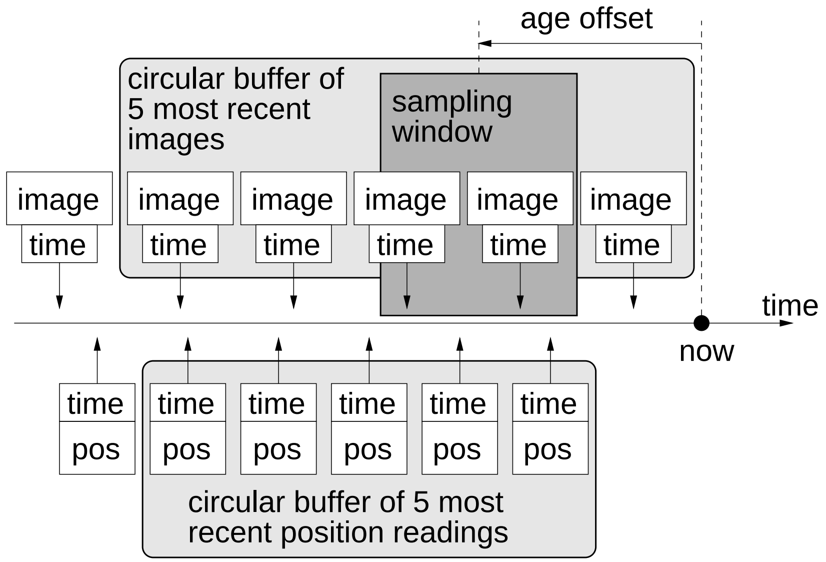

The most recent image that lies within a certain age range is selected: there will be two position readings on either side of it. The image is labelled with a position calculated by linear interpolation between the two position readings.

Temporal calibration

The time-stamps on the position readings are offset by a constant amount to account for the different latencies of the two data streams.

The user holds the probe against skin, then jerks it off suddenly. A step change is detected in the image and position streams. The offset is set so that the two changes are observed at the same time.

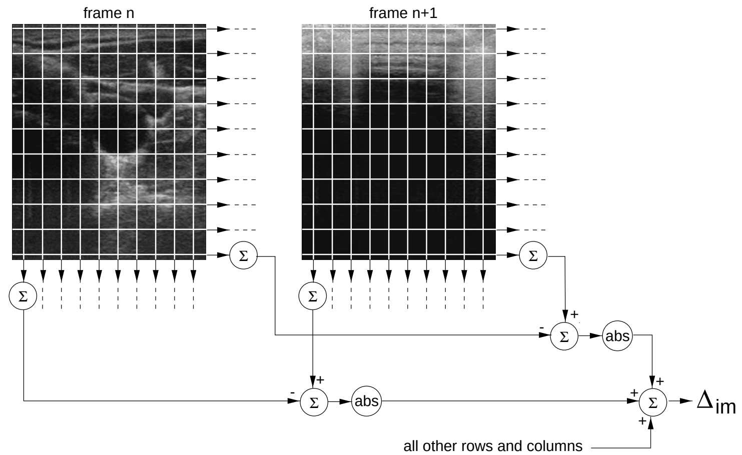

The image change is detected by comparing row and column pixel sums over consecutive frames. The position change is easily spotted directly from the position readings.

Spatial calibration

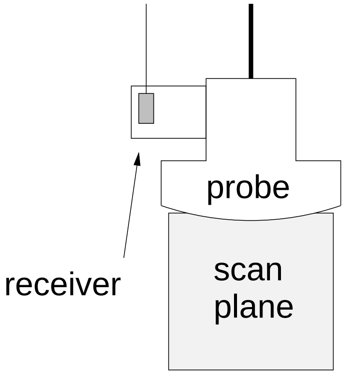

We need to work out the transformation from the position sensor's receiver to the ultrasound scan plane. It has eight parameters:

1. The x offset of the scan plane.
2. The y offset of the scan plane.
3. The z offset of the scan plane.
4. The azimuth rotation of the scan plane.
5. The elevation rotation of the scan plane.
6. The roll rotation of the scan plane.
7. The x-direction scale in the ultrasound image.
8. The y-direction scale in the ultrasound image.

Phantom-based calibration

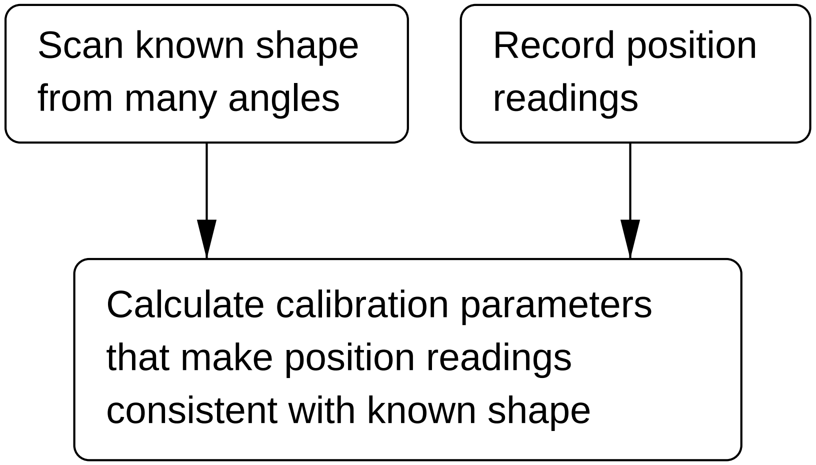

- Derive non-linear equations from the position in the images of points on the known object. Different values of the calibration parameters will make these points appear to be in different places in 3D space.
- Solve the equations iteratively to find the set of calibration parameters that places the points in 3D space in the way that is most consistent with the known object.

The cross-wire phantom

The most common calibration technique involves scanning a phantom made of wires in a water bath.

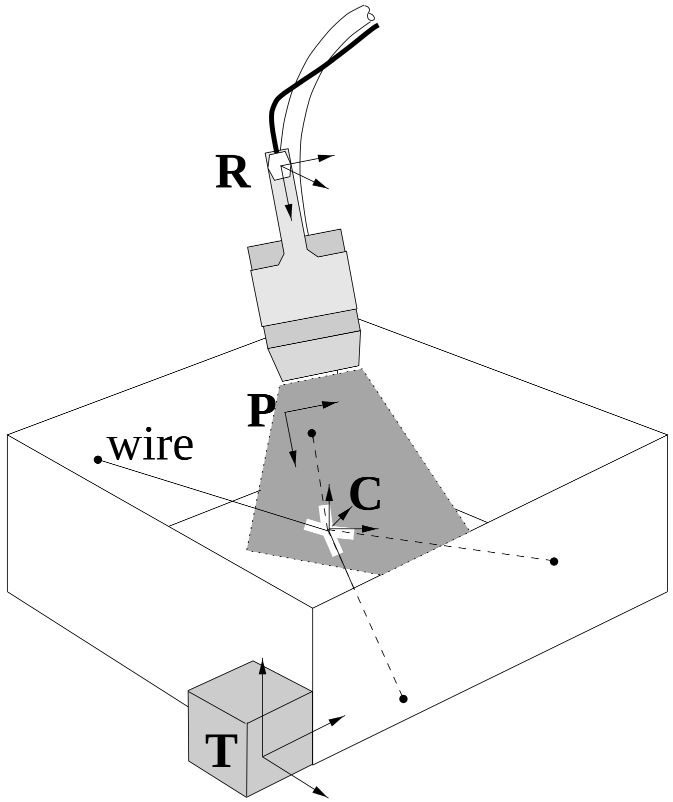

The correct calibration parameters will locate the centre of the cross at the same point in 3D space, whatever the scanning direction.

Scan of the cross-wire

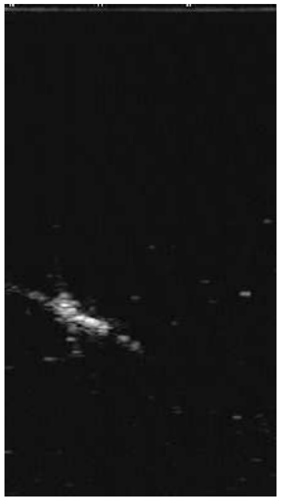

- The crossing point has to be located in the image by hand. This severely limits the number of images that can be used, which in turn limits the accuracy of the resulting calibration.
- It is hard to see where the centre of the wire is. This is because the ultrasound beam has a finite width of anything up to 1cm. There is no way of relating the position of the wires consistently to the centre of the ultrasound beam. This introduces further inaccuracy.

Calibrate on a plane

Scan the base of a water bath. This is simple, easy and cheap.

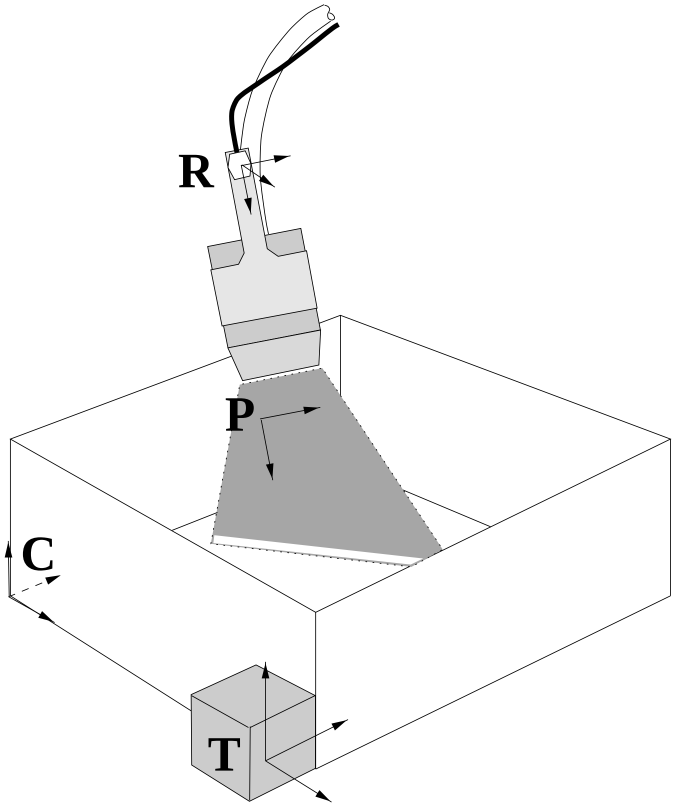

The correct calibration parameters will reconstruct the base as a plane in 3D space.

Scan of the plane

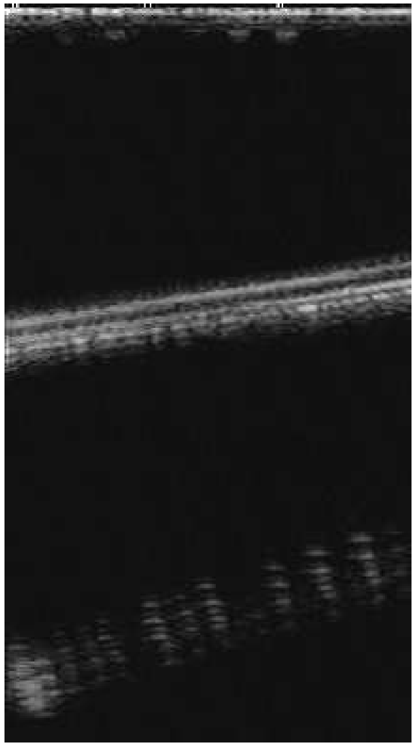

The base of the water bath can be detected automatically using standard edge detection techniques.

Automatic line detection

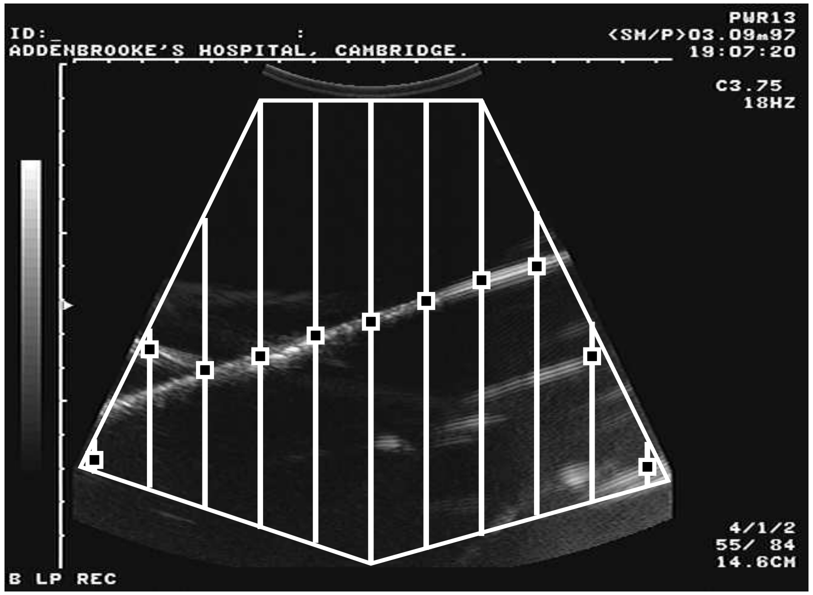

The random sample consensus (RANSAC) algorithm is used to detect the line in the image. This is more robust than least-squares.

It is perfectly feasible to use hundreds of scans in the calibration procedure.

Minimal scanning sequence

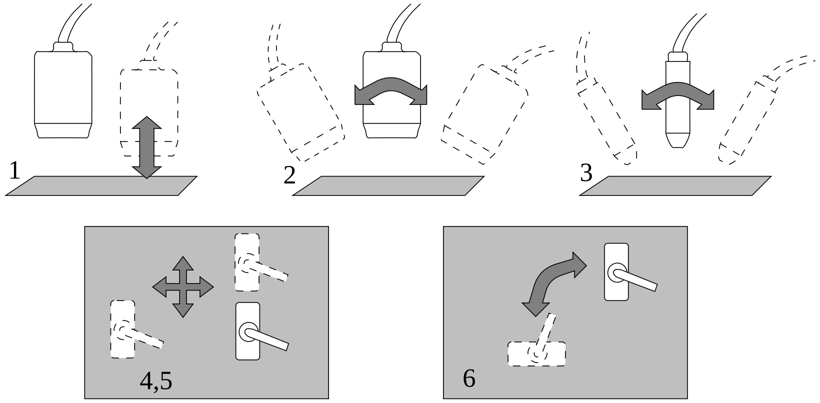

It is important to exercise all degrees of freedom of motion, otherwise some of the calibration parameters will be unidentifiable.

Beam thickness problem

Unfortunately, the beam thickness problem limits the accuracy with which we can locate the plane in the images.

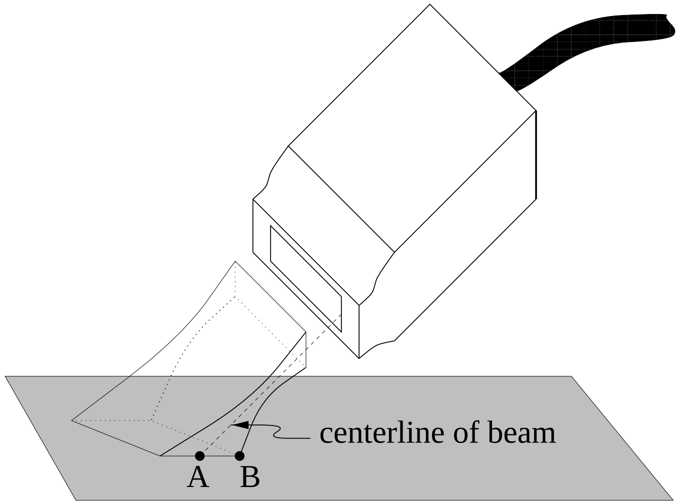

The first echo will come from point B, whereas we really want to detect point A.

There are also problems with specular reflection at glancing angles of incidence: echos from the plane are weak.

The Cambridge phantom

The Cambridge phantom overcomes these problems.

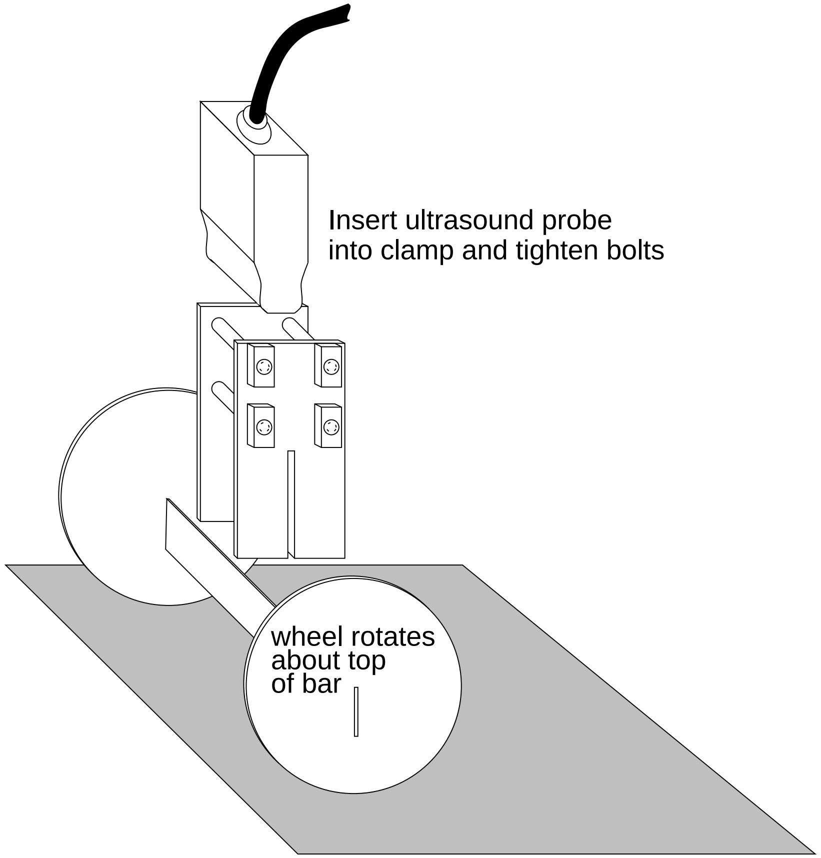

The bar traces out a virtual plane as the phantom is moved around the base of a water bath.

Scan of the Cambridge phantom

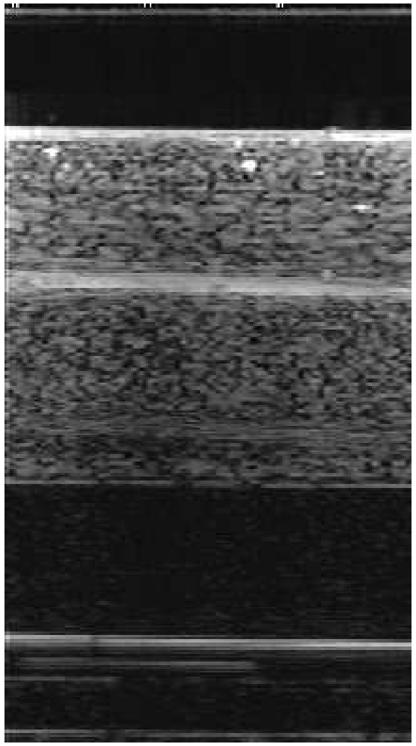

The reflection of the bar is strong, even when the assembly is rotated. The reflection comes from the centre of the ultrasound beam.

The Cambridge phantom in use

A typical calibration procedure takes less than 10 minutes in total.

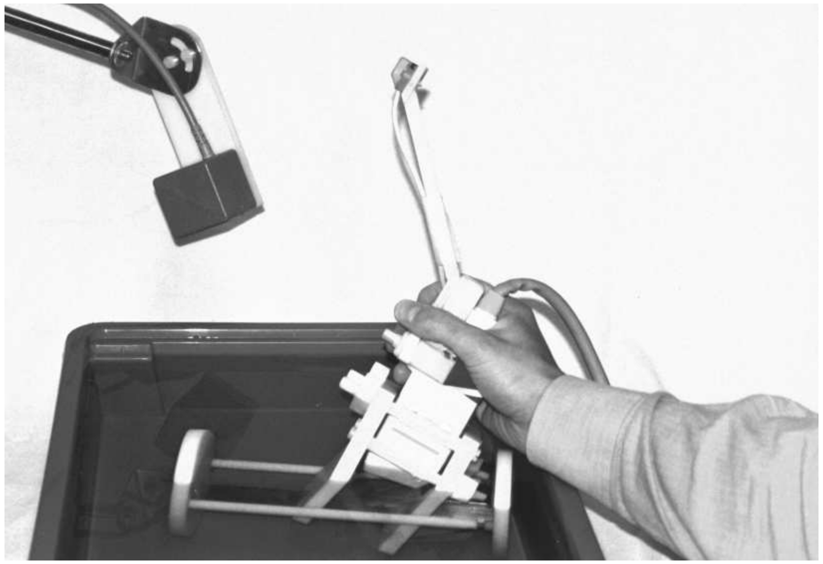

The technique is as accurate as any other technique published in the literature.

The calibration needs to be repeated when the position sensor is re-mounted on the probe, or when the clinician changes the pan and zoom settings on the ultrasound machine.

3D ultrasound acquisition summary

Freehand scanning

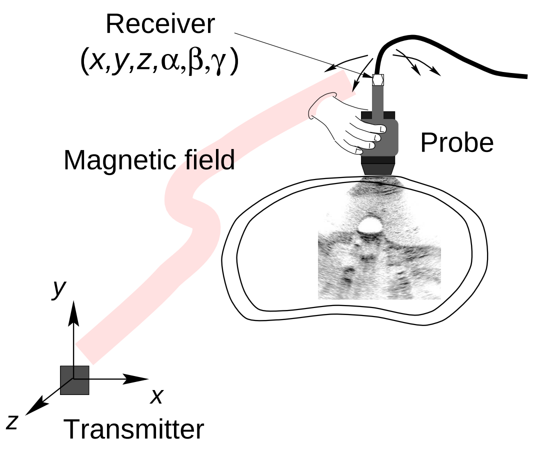

Raw 3D ultrasound data

1	B-scan image	$(x, y, z, \alpha, \beta, \gamma)$
2	B-scan image	$(x, y, z, \alpha, \beta, \gamma)$
⋮	⋮	⋮
n	B-scan image	$(x, y, z, \alpha, \beta, \gamma)$

The calibration processes ensure that we record accurate data. We will now look at how we might **visualise** the data.

Voxel arrays

Conventional 3D ultrasound reconstruction uses a **voxel array**.

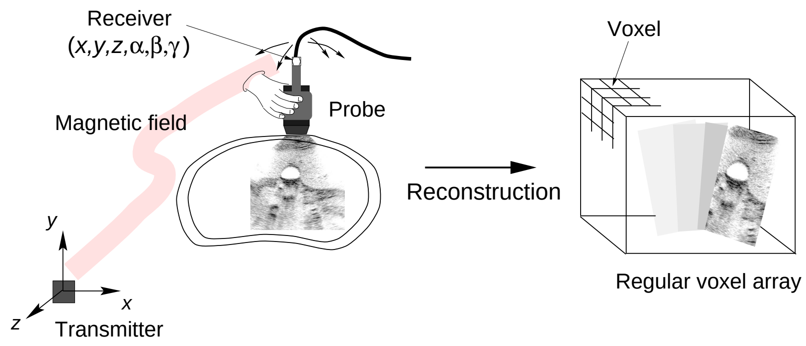

A voxel array is like a 3D picture: think of voxels as 3D pixels.

Why voxel arrays?

- Inertia — MRI and CT use voxel array.
- Relatively easy to reslice, volume render and segment.
- Efficient use of computer memory.

Using voxel arrays

The voxel array can be **resliced** (quickly) . . .

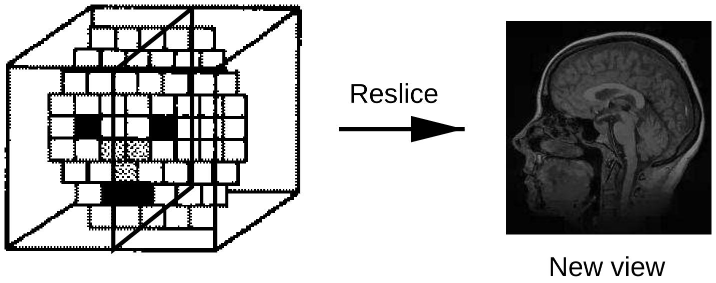

. . . or **volume rendered**.

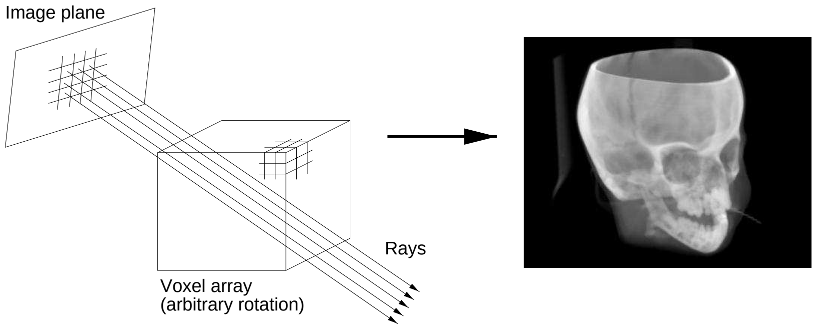

Using voxel arrays

The voxel array can be **segmented**.

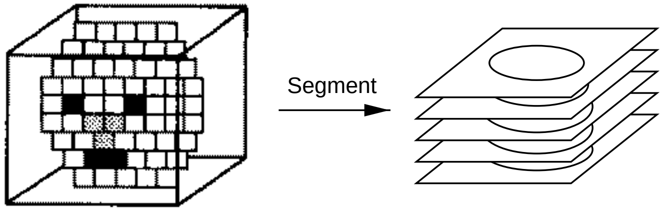

Segmentation is a prerequisite for surface rendering and volume measurement.

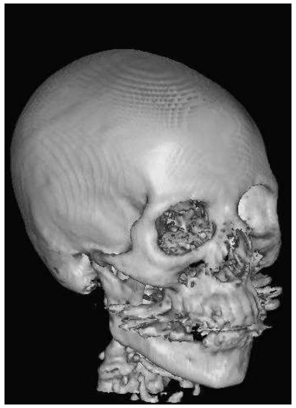

Volume = 0.856 litres

Voxel arrays from freehand 3D ultrasound

Irregularly sampled data, so . . .

- Voxels may be empty.
- Voxels may be intersected by multiple B-scans.

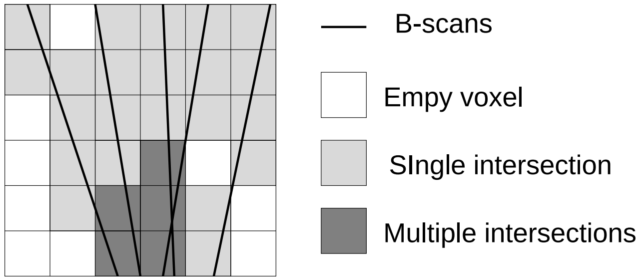

Slice through voxel array

Problems

What value do we write into voxels which are intersected by more than one B-scan?

What do we do about empty voxels? They create artifacts in reslices and volume renderings, and they make segmentation very difficult.

What size do we make the voxels?

Some common "solutions"

- Functional interpolation. Fit basis functions to the scattered data, then resample at the voxel centres — very expensive.
- Many faster, *ad hoc* approaches can be found in the literature — very arbitrary.

The better interpolation schemes account for the finite width of the ultrasound beam.

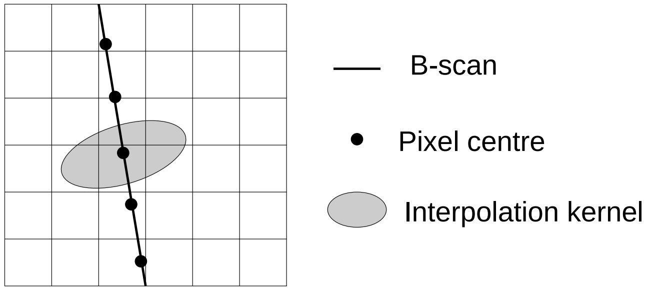

Slice through voxel array

With all voxel schemes, there are many "fudge factors" to set, the reconstruction takes time and . . .

"The images are filtered beyond recognition, as is the case with many current commercial systems."

(Anonymous referee, March 1998)

Sequential 3D ultrasound

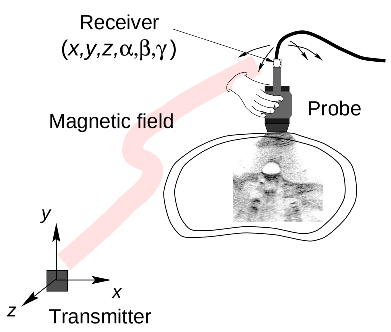

Raw 3D ultrasound data

1 B-scan image $(x, y, z, \alpha, \beta, \gamma)$

⋮ ⋮ ⋮

n B-scan image $(x, y, z, \alpha, \beta, \gamma)$

From the raw data, we can *directly* obtain:

- Reslices
- Segmentations (and volume measurements)
- Volume renderings

Advantages:

- No fudge factors
- No delays
- Less filtering

Sequential vs. voxels

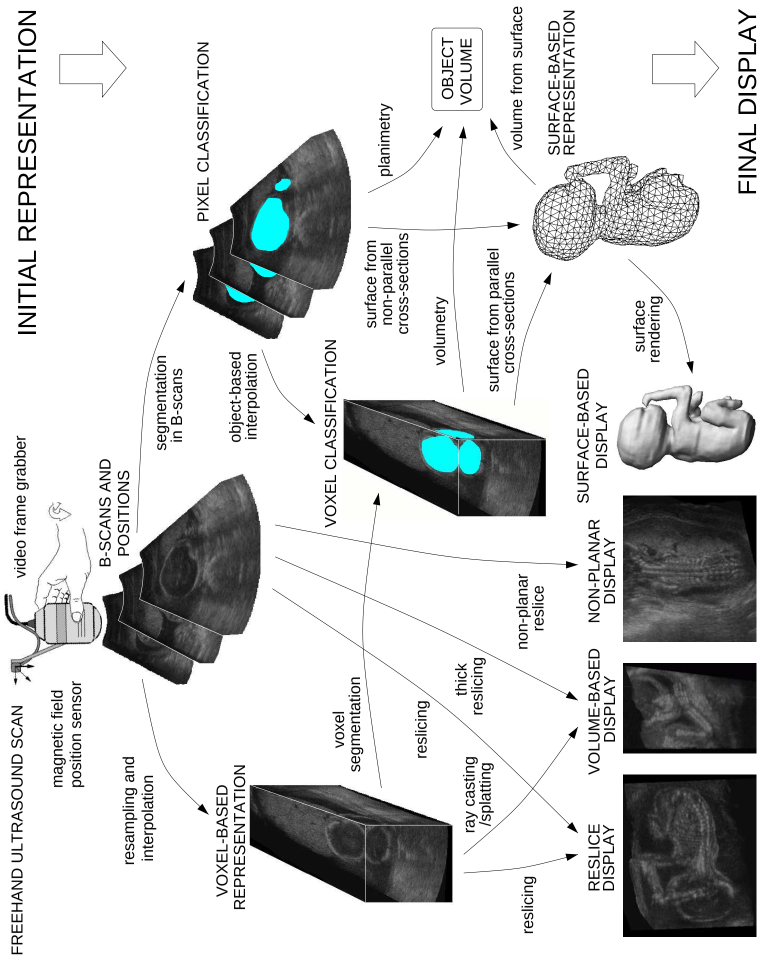

Sequential algorithms bypass the voxel array stage.

Sequential reslicing

Naive approach:

- Find the line of intersection of each B-scan with the slice plane.
- Extract grey level intensities along this line.
- Paint the intensities onto the slice plane.

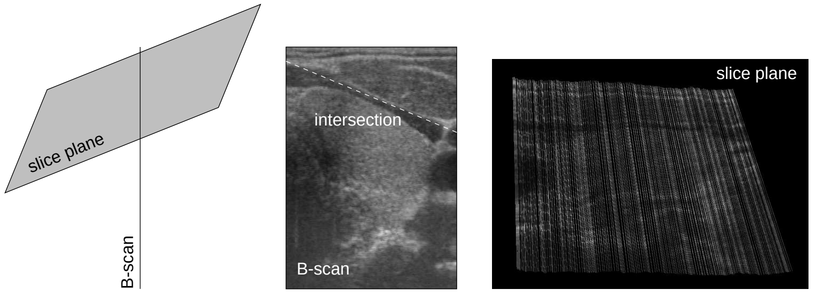

(a) (b) (c)

- The slice comprises a set of line segments.
- We need to fill the gaps.
- We can do better than standard interpolation between the line segments.

Sequential reslicing

The gap filling scheme should account for the finite beam width.

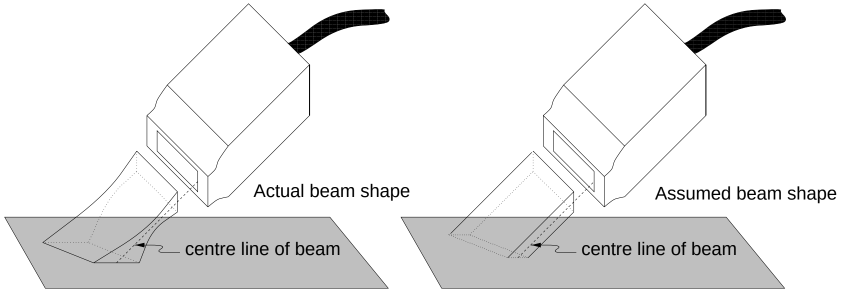

The intersection of the slice plane with each "fat" B-scan is now a polygon.

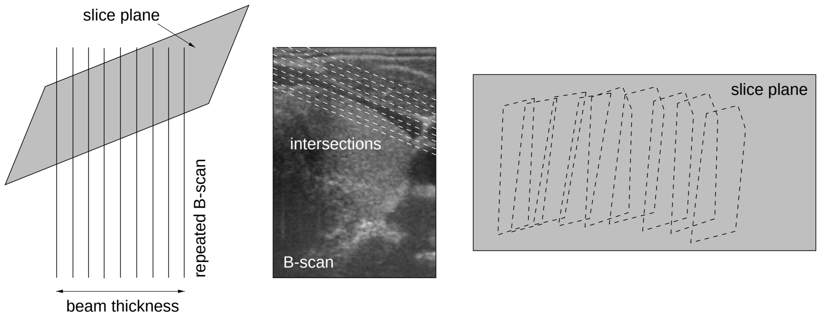

(a) (b) (c)

The slice plane is tiled with a set of overlapping polygons, all filled with grey level intensities.

Sequential reslicing

Question: Which intensity should be displayed at places where two or more polygons overlap?

Answer: The one sampled nearest the centre line of the ultrasound beam.

So paint the intensities onto a wedge, not a flat polygon.

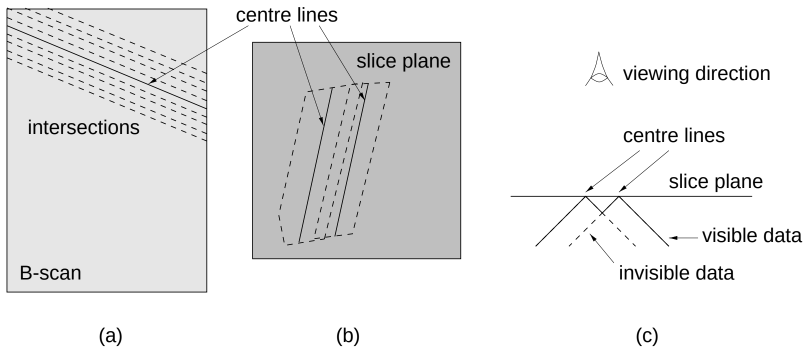

Tell the graphics system to remove hidden surfaces.

The reslicing algorithm is:

- Effectively free from parameters.
- Fast — exploits standard graphics hardware (texture mapping or Gouraud shading).

Sequential reslicing

Compare sequential slices (d)–(f) with corresponding slices through a voxel array (a)–(c).

The voxel array took several minutes to construct on a good workstation, with simple interpolation.

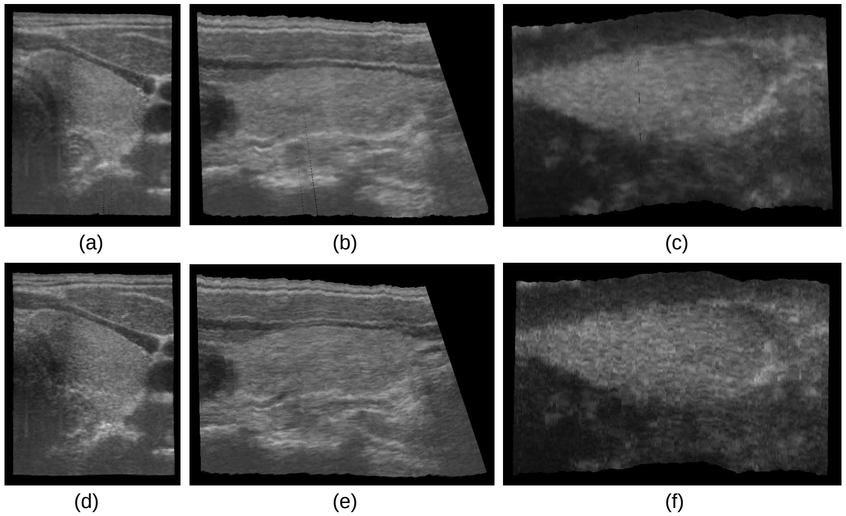

Sequential scheme needs only one B-scan at a time (in any order) and uses only the graphics buffers.

So it can be done in real-time, as the clinician performs the scan.

Reslice gallery

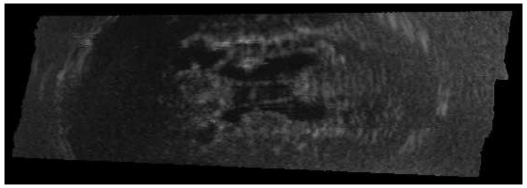

neonate's ventricles and cysts (scanned through fontanelle)

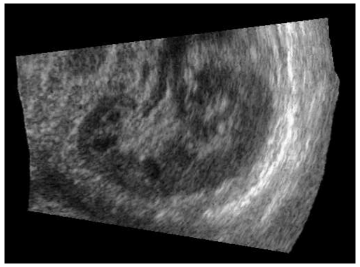

coronal kidney

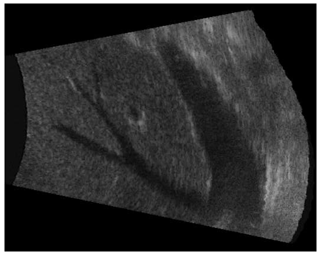

hepatic veins and IVC

22-week fetus

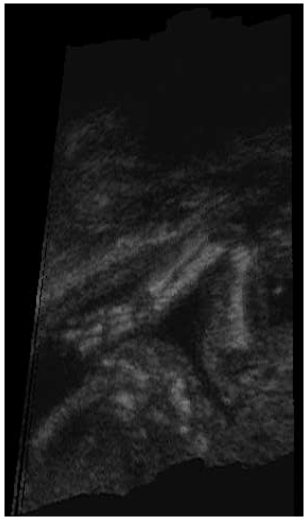

22-week fetus

Non-planar reslicing

Non-planar reslicing is also possible. The user specifies a developable surface, which is 'painted' with the data it intersects. The painted surface is then flattened out for display on a flat screen.

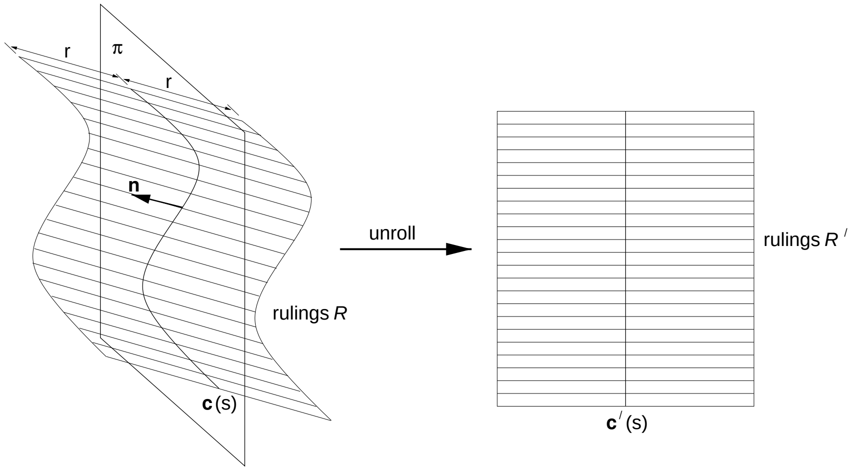

developable surface non-planar reslice image

The surface is defined by a reslice plane $\boldsymbol{\pi}$ and a plane curve $\mathbf{c}(s)$ drawn in $\boldsymbol{\pi}$. The surface is swept out by the set of **rulings** $\mathcal{R}$ of length $2r$, which are normal to $\boldsymbol{\pi}$ and intersect $\mathbf{c}(s)$ at their midpoints.

The non-planar reslice is constructed in a sequential framework. Care is taken to preserve distances.

Constructing the non-planar reslice

- Calculate the pixel dimensions of the non-planar reslice image. These can be deduced from $\mathbf{c}(s)$, r and the scale factor (mm/pixel) of the B-scans.
- Use the scaling again to locate in 3D space each pixel of the non-planar reslice image.

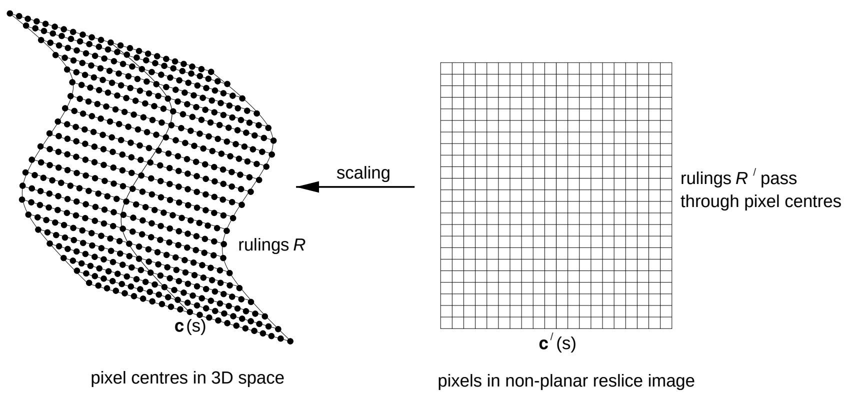

- Shade each pixel according to the intensity of the nearest B-scan pixel, but do not search beyond a distance d for the nearest B-scan pixel.
- Areas of the surface which are a long way from any recorded data are left blank, and not interpolated with misleading data.

Efficient sequential implementation

- Consider each B-scan in turn.

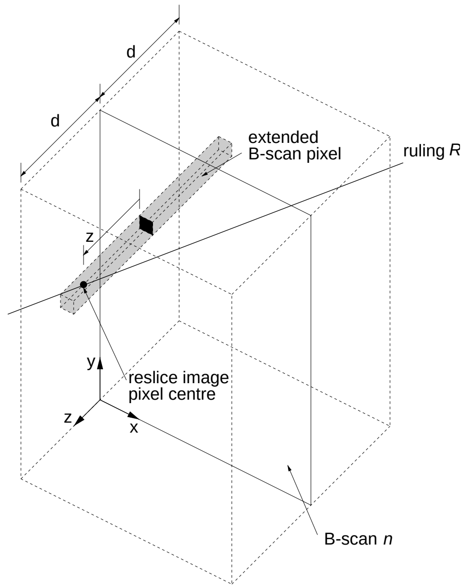

- Each extended B-scan pixel containing one of the reslice image pixels is a candidate for shading the reslice image pixel: it is the closest pixel on B-scan n and lies within the distance limit d.
- Render the reslice image pixel with the intensity of the extended B-scan pixel, *at a depth* $|z|$.
- Should a pixel in a future B-scan be closer, the reslice image pixel will be rendered again at a shallower depth, overwriting the old value.

Efficient sequential implementation

- The fronto-parallel view reveals how the intersection tests can be performed efficiently.

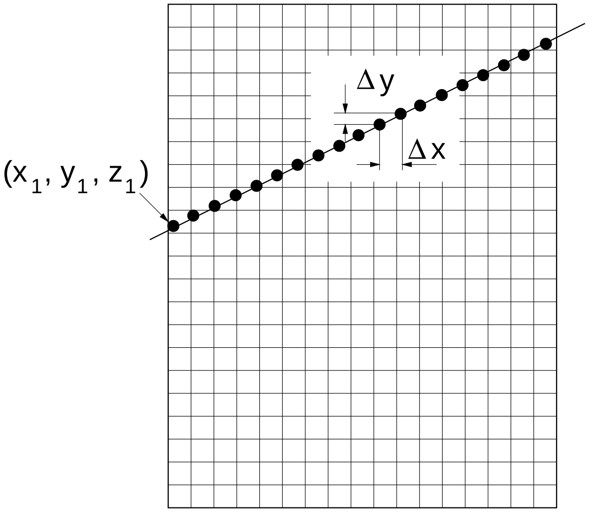

Δz into the page

- For each ruling in $\mathcal{R}$, locate only the first intersection (x_1, y_1, z_1) to sub-pixel accuracy, and determine the increments Δx, Δy and Δz.
- Then repeatedly add the increments to (x_1, y_1, z_1), rounding down the x and y values to locate the intersected B-scan pixels.

Example: 16-week foetus's leg

The length of the flattened leg is about 75mm.

- The slider controls the interpolation limit d.
- Resize the window to change the width r.

Example: 22-week foetus's spine

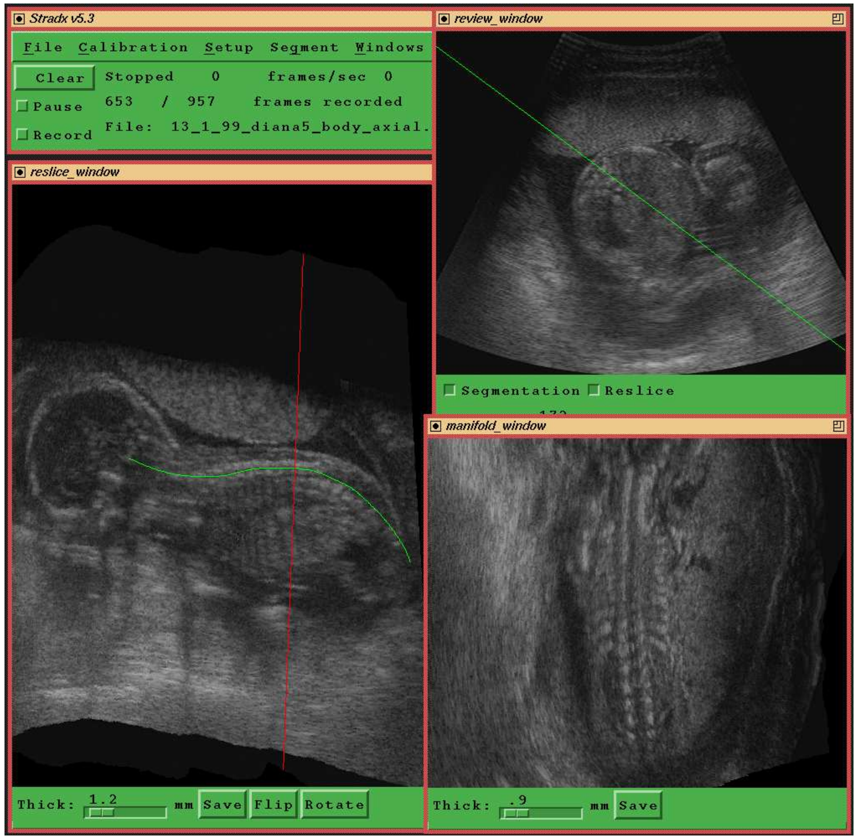

The length of the flattened spine is about 117mm.

Volume rendering

- Volume rendering can also be performed in the sequential framework, by blending together a number of parallel reslices.

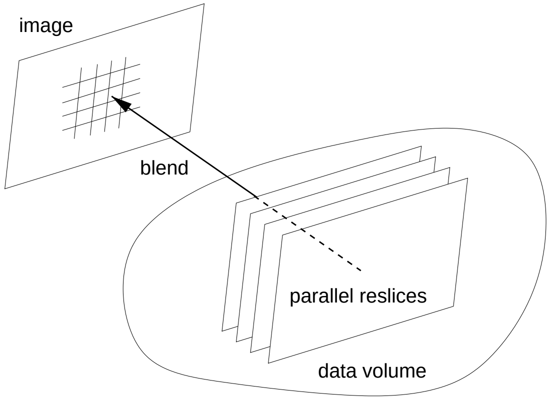

The blending can be performed in three ways:

- **Maximum intensity compounding** highlights bright structures like bone.
- **Minimum intensity compounding** highlights dark structures like blood vessels.
- **Average compounding** reduces the visibility of speckle noise.

Maximum intensity compounding

- The user sets up the volume rendering by specifying a standard reslice plane and a thickness.
- Compare the standard, thin reslice (left) with the 14mm thick reslice (right).

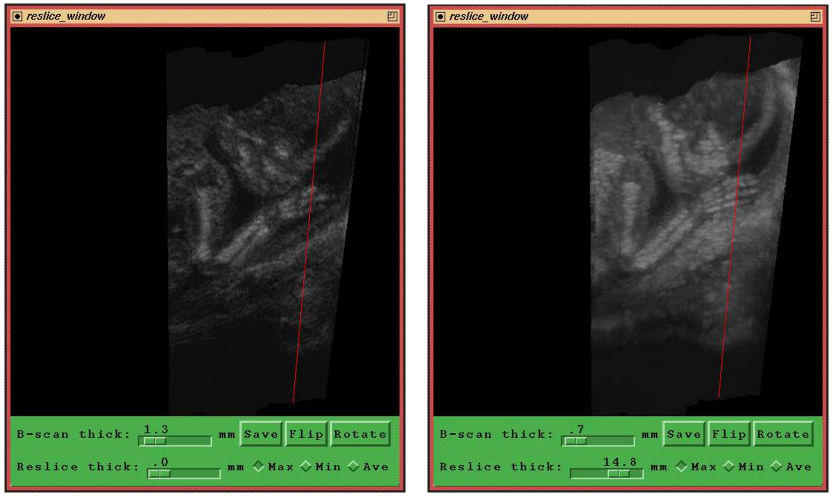

- The bone structure of the foetus's hand is much more clearly visible in the volume rendering.
- It was not necessary to take particular care in positioning the reslice plane.

Average compounding

- Compare the standard, thin reslice (left) with the 13mm thick reslice (right).

- The averaging has reduced the level of speckle noise.
- The foetus's spine and ribcage are much more clearly visible.

Non-planar volume rendering

- Volume renderings can also be constructed by blending together *non-planar* reslices.

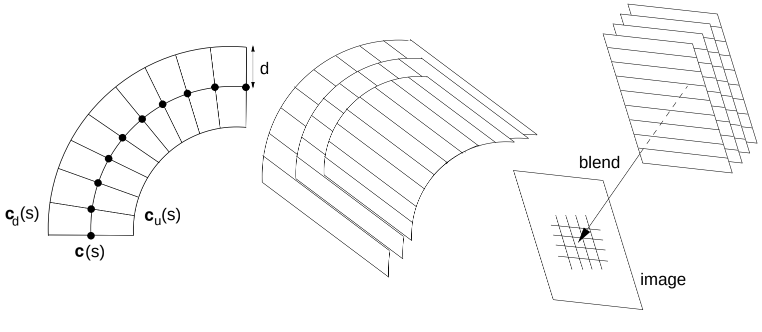

(a) contours and rulings (b) surfaces (c) unrolled surfaces and volume rendering

Example: a 16-week foetus's skeleton unrolled.

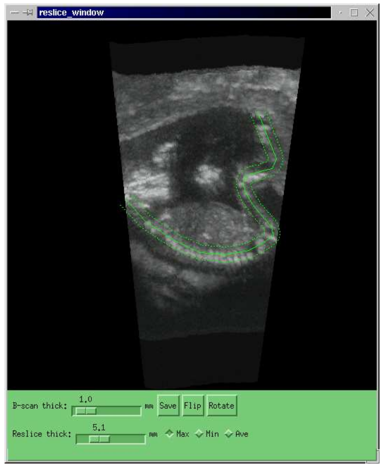

thick planar reslice

thick non-planar reslice

Panoramas

- Similar techniques can be used for panoramas.
- Like Siemens Siescape, but cheaper!

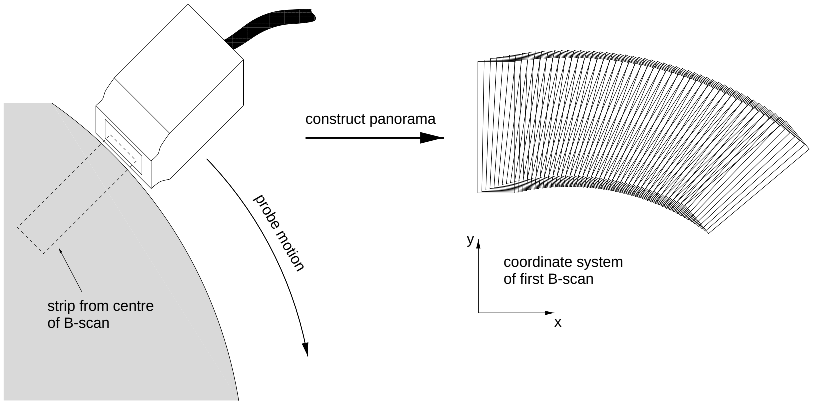

- Move the probe in the plane of the B-scans.
- Extract a narrow strip from centre of B-scan.
- Stitch together to make a seamless composite.
- Use position sensor readings to register B-scans.
- Siemens use image-based correlation.

Panoramas

For each pair of B-scans, find θ and $(\delta x, \delta y)$. Concatenate to refer back to first B-scan.

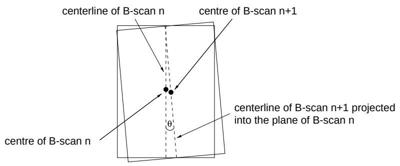

Use wedges to deal with overlaps.

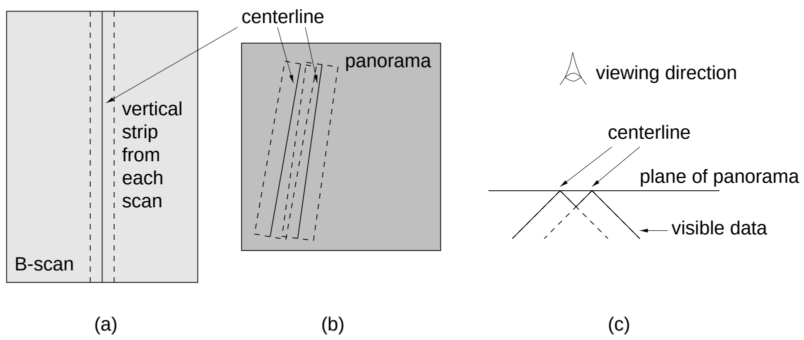

Can set strip width automatically for no gaps.

So no parameters, no memory $\rightarrow$ real-time.

Panorama gallery

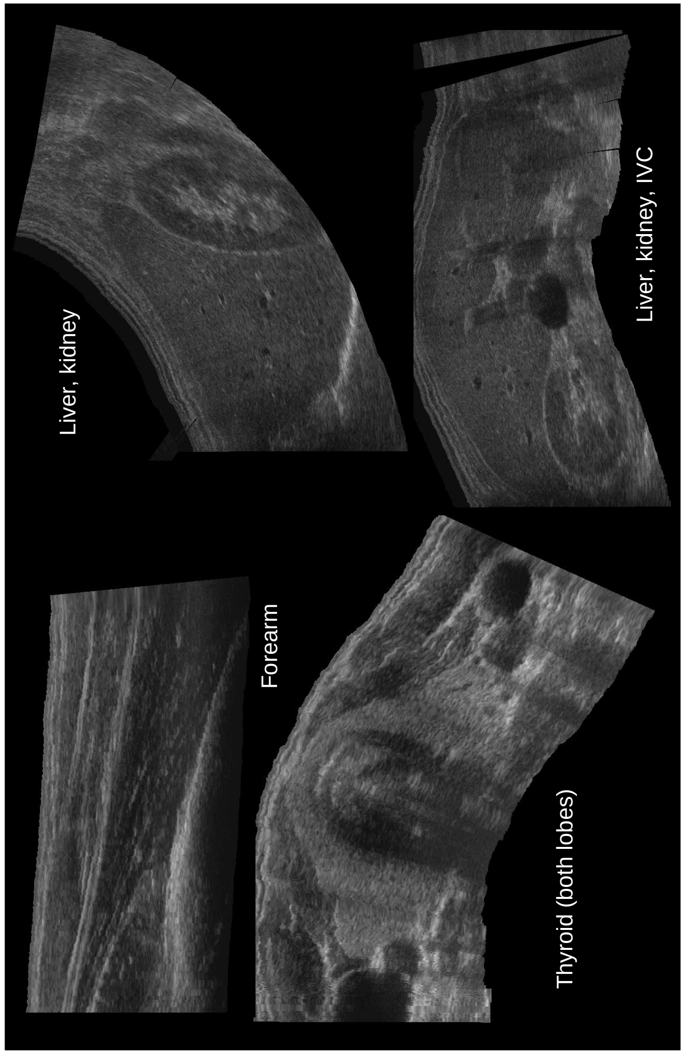

Volume measurement

Objectives:

- To measure the way structures change in size during the progression of a disease.
- To assess response to treatment through changes in the volumes of structures.
- To provide accurate volumes for calculating drug dosage and planning treatment.

Current clinical practice often involves the use of formulae based on the volume of an ellipsoid, modified by various fudge factors. These estimates can be in error by over 20% in some cases.

Sequential 3D ultrasound offers the possibility of a more accurate technique, fast enough to be completed while the patient is present at the clinic.

Before a volume can be estimated, it is first necessary to **segment** the structure of interest. This is by far the trickiest and most time-consuming step.

Manual segmentation

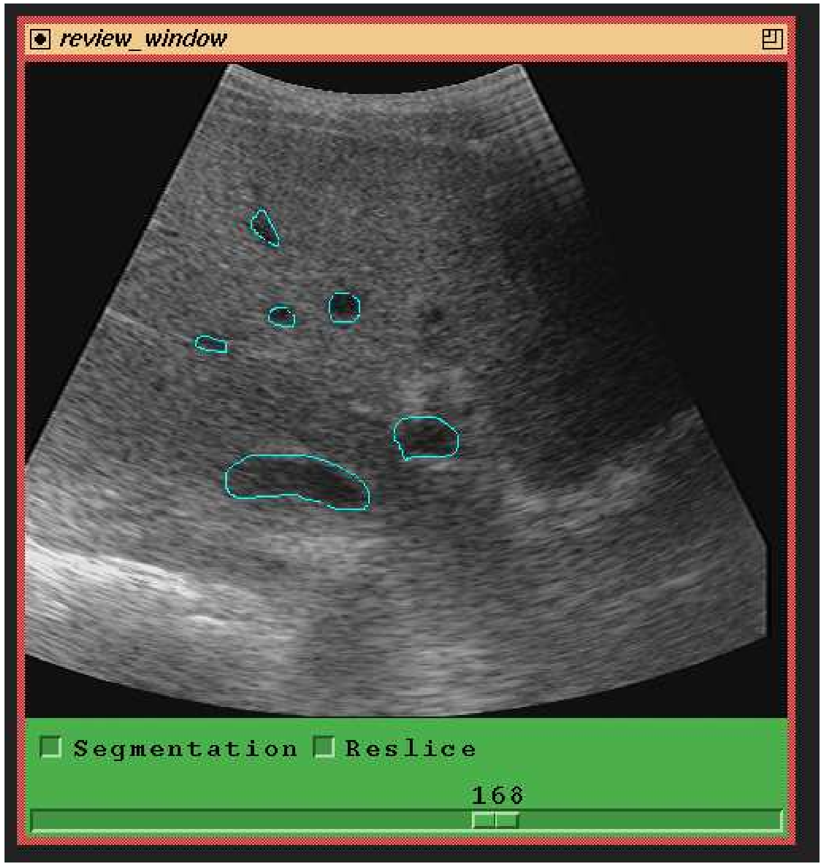

Segmentation can be performed by drawing around the structures of interest in the original B-scans. This is slow, but reliable.

Manual segmentation

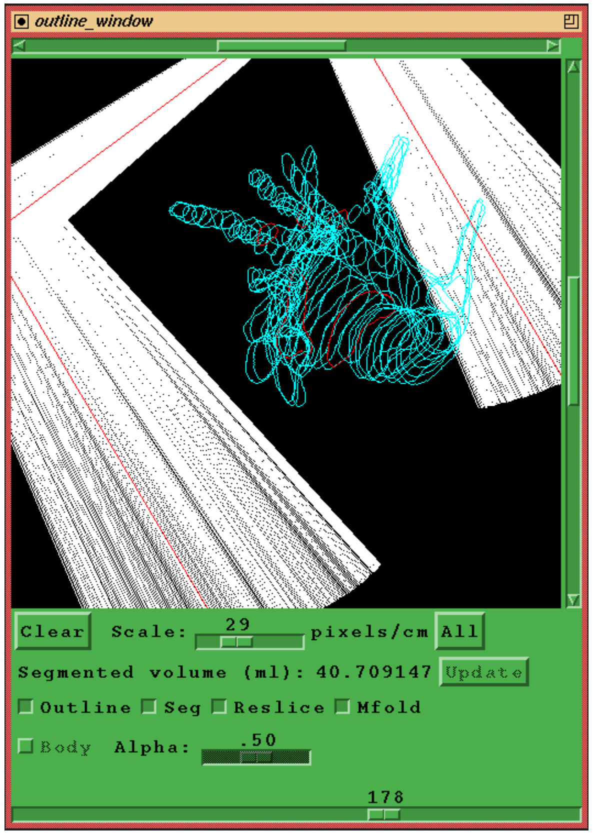

After several B-scans have been segmented, it is possible to estimate the volume using one of two techniques: **cubic planimetry** and **shape-based interpolation**.

Volume measurement overview


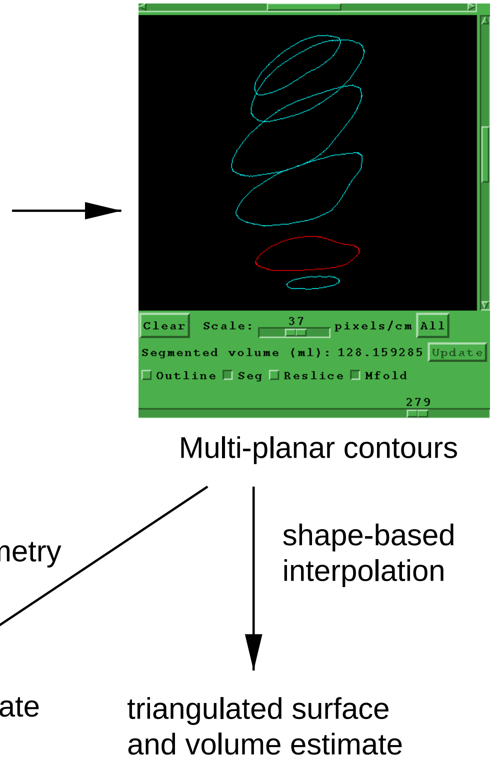

Cubic planimetry

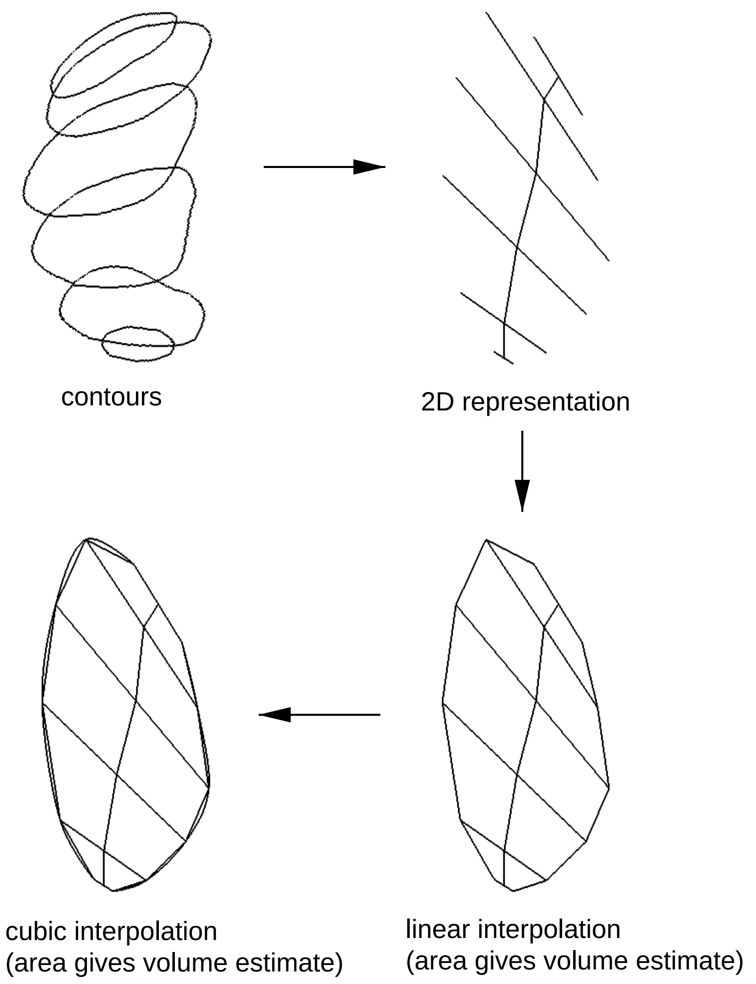

Shape-based interpolation

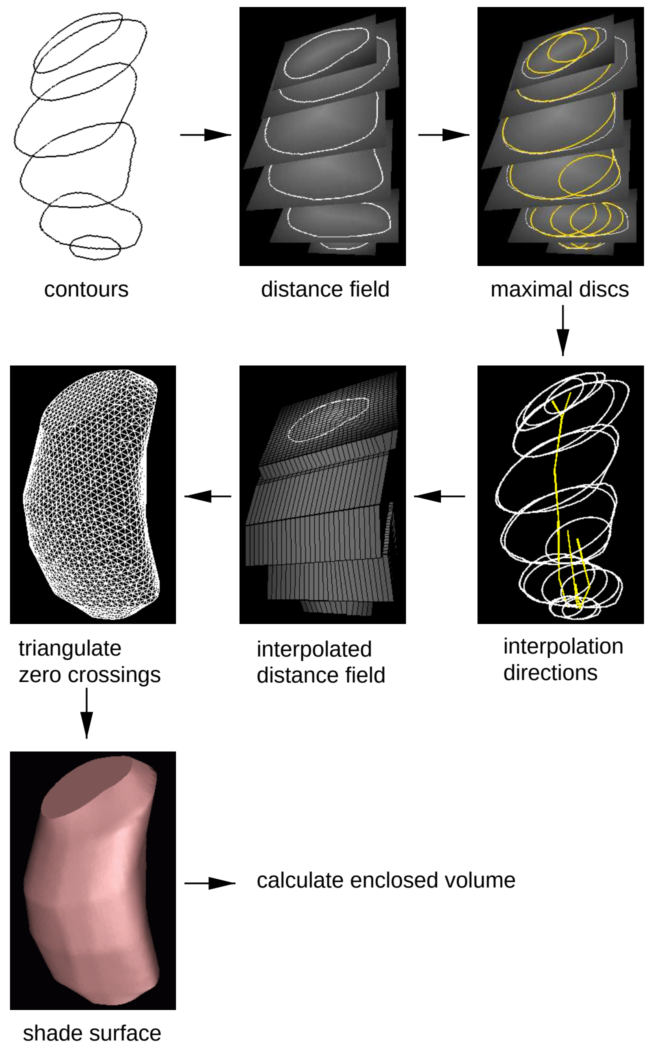

Shape-based interpolation

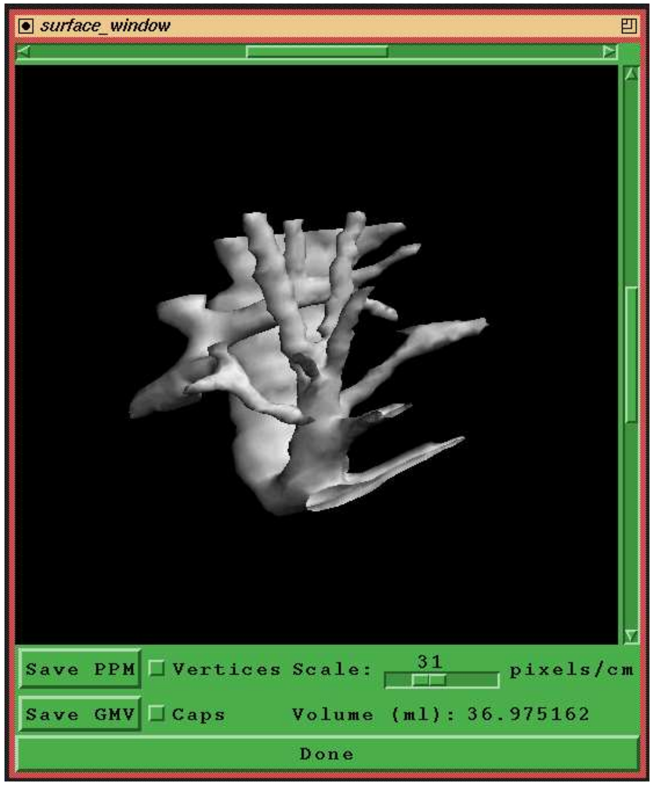

Here's the hepatic system reconstructed using shape-based interpolation. *In-vivo* experiments have shown the volume estimate to be accurate to within 5% of the true value. Only a sparse set of cross-sections is required.

Shape-based interpolation

- Another example of shape-based interpolation.

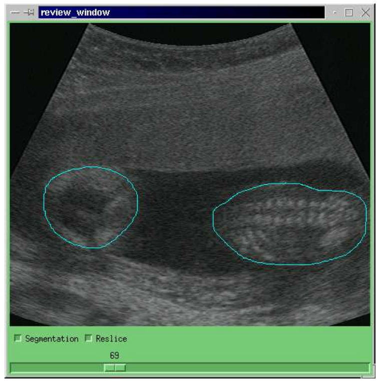

Head and torso B-scan

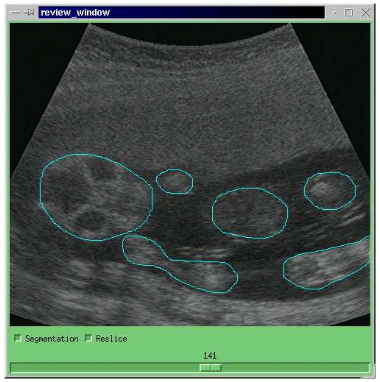

Head, torso and limbs B-scan

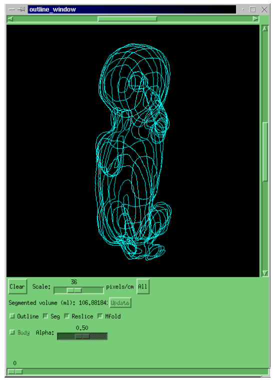

'Outline' window

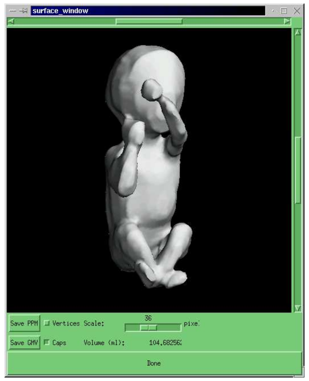

'Surface' window

Segmenting large structures

- Cross sections of large structures (like the liver) do not fit in a single B-scan.
- Multiple sweeps of the probe are required to scan large structures in their entirety.

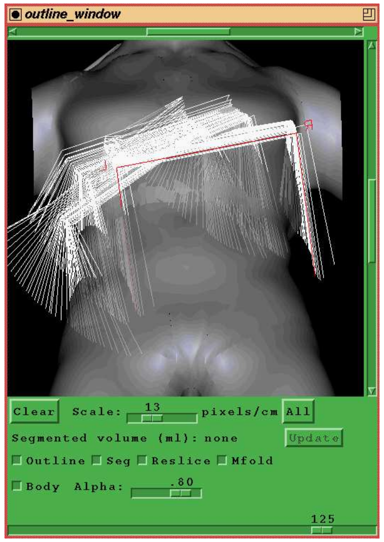

Three sweeps

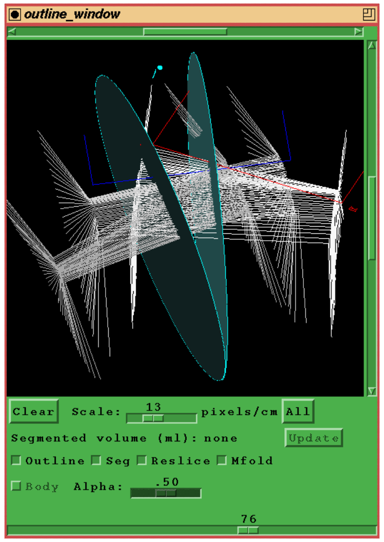

Two dividing planes

- Space can be partitioned using *dividing planes*. In the example above, we have three partitions and two dividing planes.
- Each of the three partitions is associated with a particular sweep.

Segmenting large structures

- The B-scans are segmented by hand as before, except now only part of a cross-section is visible in each B-scan.
- The user therefore traces *open* curves in the B-scans.

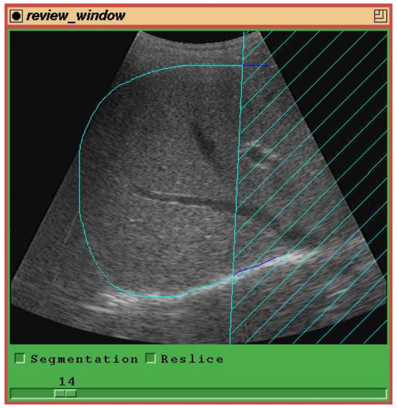

Segmentation in partition 1

Segmentation in partition 2

- The shaded areas correspond to another partition which is best segmented in another sweep.
- It is only necessary to trace the boundary in the unshaded areas.

Segmenting large structures

- Each sweep yields a segmentation for one partition of space.
- Cubic planimetry can be used to provide a volume for each partition, then summed to find the total volume (below left).

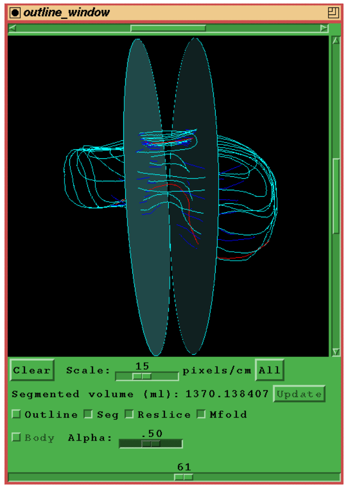

Combined contours

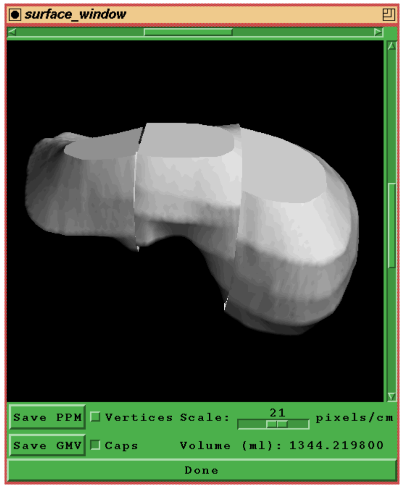

Combined surfaces

- Shape-based interpolation can be used to fit a surface in each partition.
- The surfaces are then combined to visualise the entire structure (above right).

Visualising large structures

- Dividing planes can also help when reslicing large structures.
- If resliced in the usual way, mis-registration artefacts are apparent where one sweep overlaps another.
- Also, the black background of one sweep interferes with the ultrasound data in another.

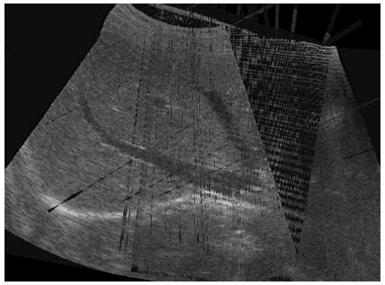

Without dividing planes

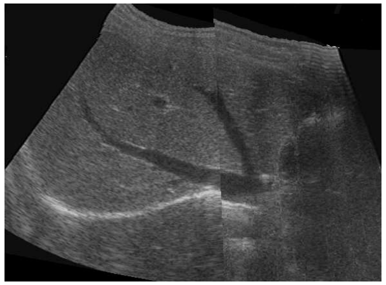

With dividing planes

- With dividing planes, only one sweep is used in each partition.
- The mis-registration is still apparent, but the reslice is certainly intelligible.

3D Doppler ultrasound

Stradx can also record colour Doppler data using only one byte per pixel. The pixels are coded on-the-fly using luma and chroma thresholds to classify pixels as coloured or greyscale.

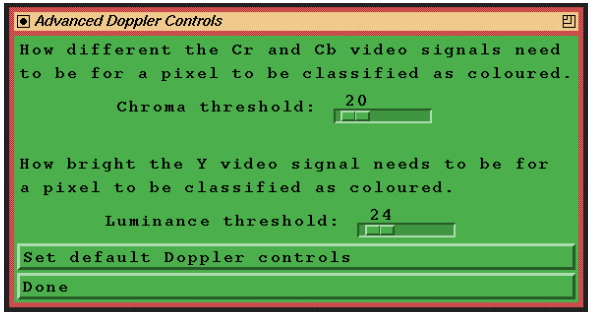

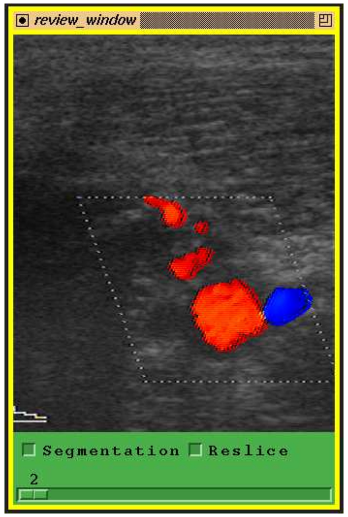

The thresholds are correct when the image in Stradx's preview window matches the image on the ultrasound machine's screen.

Visualising colour data

Colour data can be visualised in precisely the same way as greyscale data. This includes reslicing . . .

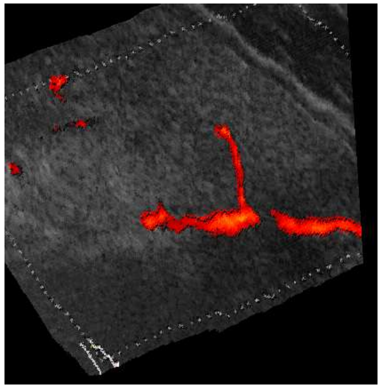

. . . and panoramas . . .

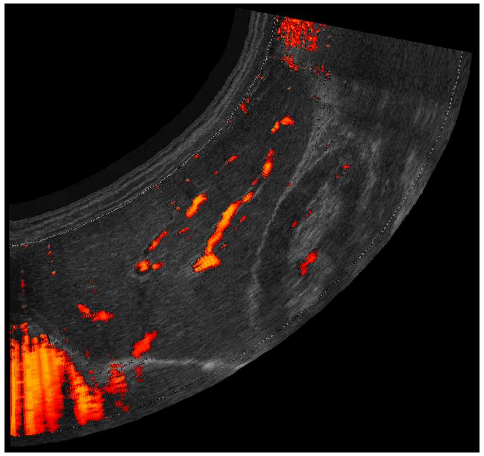

Visualising colour data

. . . and volume renderings . . .

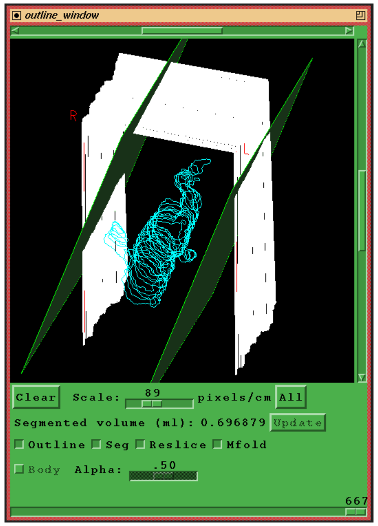

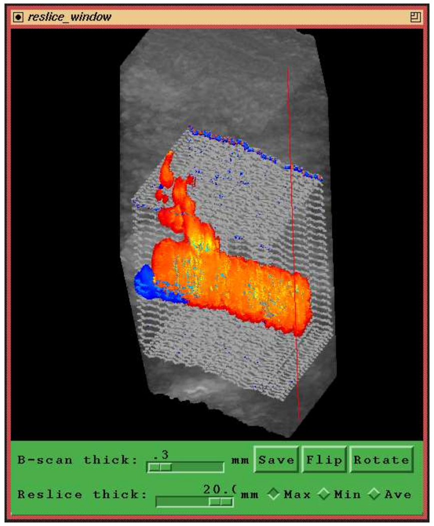

- The 'Outline' window (left) shows a set of segmentation contours around the blood vessels, and the limits of the 20mm volume rendering.
- The volume rendering itself is on the right: note the bifurcations in the artery (red), and the vein (blue) hidden behind the artery.
- The stripple artefact is caused by the Doppler region-of-interest displayed on the ultrasound machine's screen.

Segmentation by thresholding

3D Doppler ultrasound data sets are relatively easy to segment by thresholding.

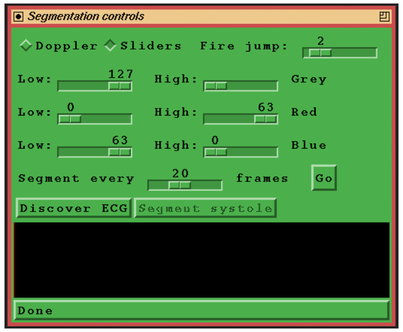

The user interactively selects the range of colours to be segmented, which are highlighted in magenta in all Stradx data windows.

In this example, the user has selected all the red pixels in the B-scan.

Semi-automatic segmentation

Some input is still required by the user, to:

- Indicate which structures are to be segmented.
- Smooth over any noise or Doppler drop-out.

The user just clicks on each blob to be segmented. A "grassfire" algorithm is used to fit a contour to the edge of the blob. The user can control how far the fire can jump (to cope with noise) and can edit the contours by hand if necessary (rare).

This segmentation required only four mouse clicks. Note how the grassfire algorithm has dealt with the signal drop-out, by jumping over small clusters of grey pixels.

Pulsatile motion and gating

The user should segment B-scans from the same point in the cardiac cycle to cope with the pulsatile motion of the blood vessels.

Stradx provides a facility to estimate the ECG signal (by counting coloured pixels) and automatically segment all thresholded pixels at systole.

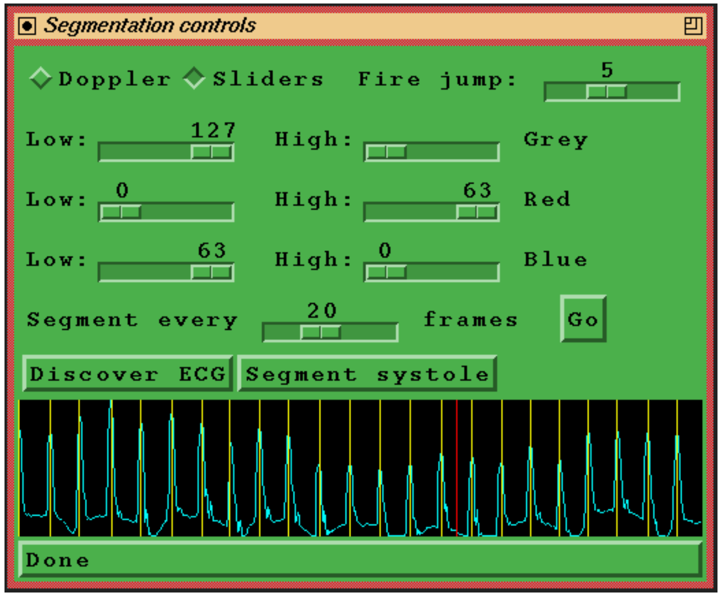

Pulsatile motion and gating

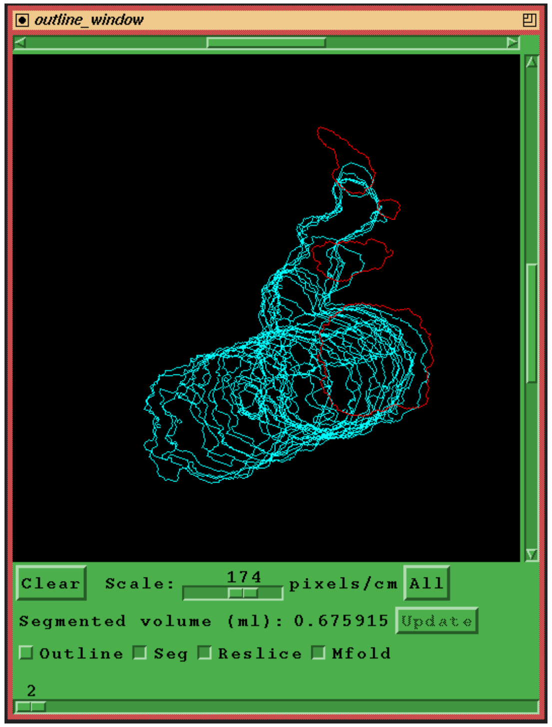

Here are the segmented vessels in the outline window. They are really tiny: the segmented volume is less than 0.7ml. The systole segmentation was entirely automatic.

Pulsatile motion and gating

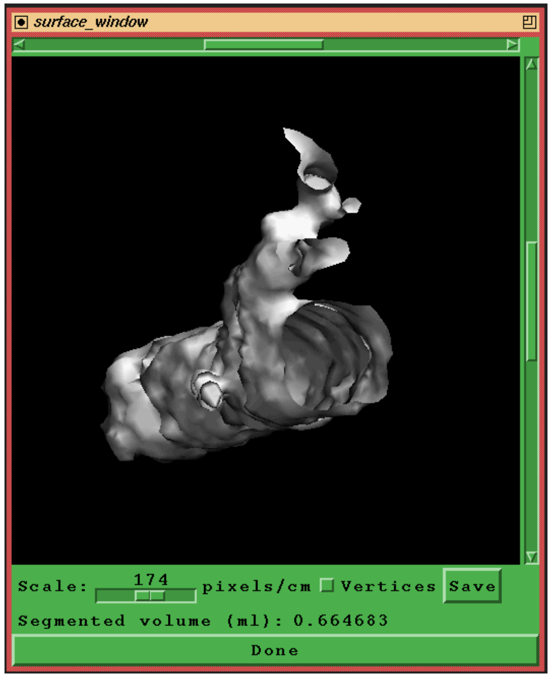

Here's a surface rendering of the segmented vessel, generated using shape-based interpolation. The rendering and both volume estimates are available *within one minute of completing the scan*.

Body-centered visualisation

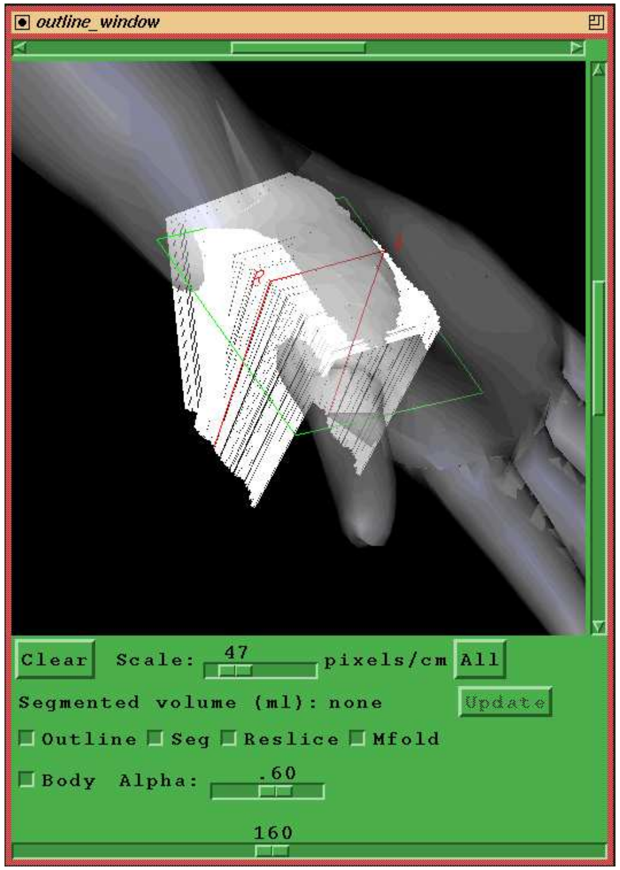

Stradx can display the data superimposed on a rendering of the human body, so there can be no doubt where the data came from.

Correcting probe pressure artefacts

- Varying the probe pressure during the scan dynamically deforms the anatomy, leading to reconstruction artefacts.
- These are particularly pronounced with high resolution scans. Here are some typical reslices:

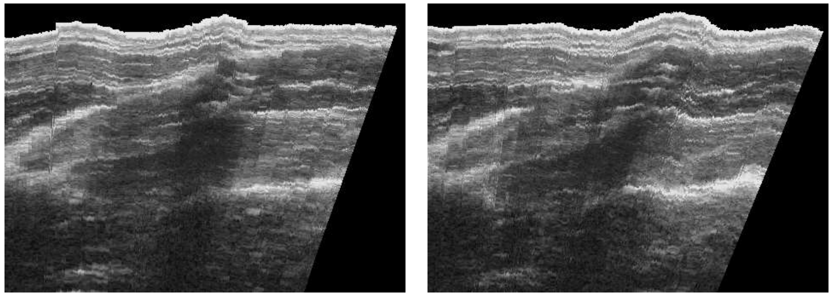

- Stradx's image correlation algorithms can compensate for varying probe pressure by repositioning and warping the B-scans:

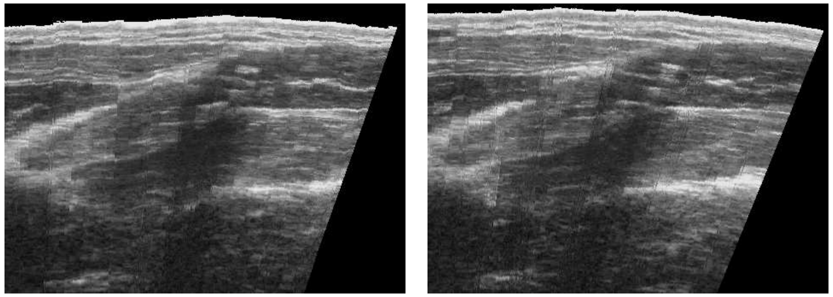

Correcting probe pressure artefacts

The compensation can also be applied to panormic data sets. Here's a thyroid before compensation . . .

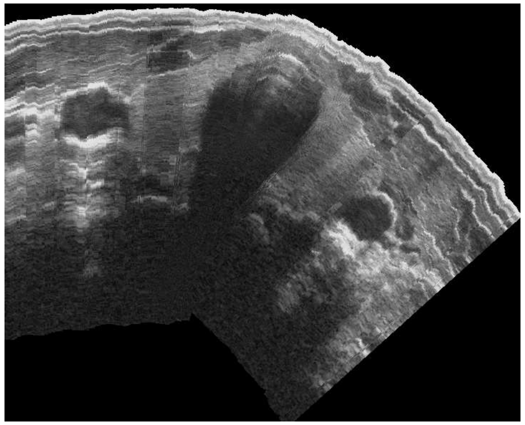

. . . and after compensation . . .

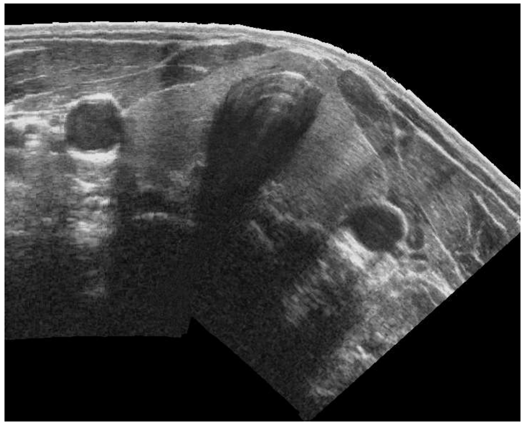

Conclusions

Stradx version 6.2 offers:

- 3D ultrasound acquisition (greyscale or Doppler).
- State-of-the-art (and easy) calibration.
- Instant reviewing, reslicing, volume rendering and panoramas.
- Manual and semi-automatic segmentation.
- State-of-the-art volume measurement and surface fitting tools.
- Probe pressure artefact removal.
- Body-centered visualisation facilities.

You'll need an ultrasound machine, a Linux PC or an SGI workstation, and a position sensor (Polaris, Polhemus or Bird). Download for free from:

`http://svr-www.eng.cam.ac.uk/~rwp/stradx/`

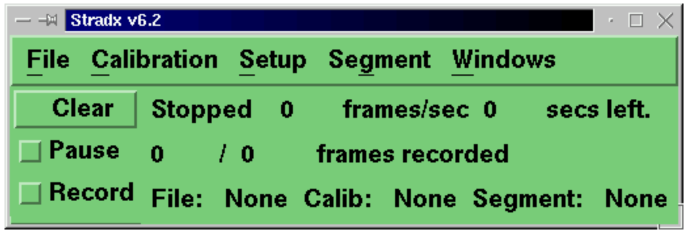

Bibliography

The following publications directly relate to the Stradx system.

A. H. Gee, R. W. Prager, G. M. Treece and L. Berman. Engineering a freehand 3D ultrasound system. To appear in *Pattern Recognition Letters*.

G. M. Treece, R. W. Prager, A. H. Gee and L. Berman. 3D ultrasound examination of large organs. *Medical Image Analysis*, 5(1):41-54, March 2001.

G. M. Treece, R. W. Prager, A. H. Gee and L. Berman. Surface interpolation from sparse cross-sections using region correspondence. *IEEE Transactions on Medical Imaging*, 19(11): 1106-1114, November 2000.

P. M. Tuomola, A. H. Gee, R. W. Prager and L. Berman. Body-centered visualisation for freehand 3D ultrasound. *Ultrasound in Medicine and Biology*, 26(4):539-550, June 2000.

G. M. Treece, R. W. Prager and A. H. Gee. Regularised marching tetrahedra: improved iso-surface extraction. *Computers and Graphics*, 23(4):583-598, 1999.

G. M. Treece, R. W. Prager, A. H. Gee and L. Berman. Fast surface and volume estimation from non-parallel cross-sections, for freehand 3-D ultrasound. *Medical Image Analysis*, 3(2):141–173, 1999.

R. W. Prager, A. H. Gee and L. Berman. Stradx: real-time acquisition and visualization of freehand three-dimensional ultrasound. *Medical Image Analysis*, 3(2):129–140, 1999.

R. W. Prager, R. N. Rohling, A. H. Gee and L. Berman. Rapid calibration for 3-D freehand ultrasound. *Ultrasound in Medicine and Biology*, 24(6):855–869, July 1998.

G. M. Treece, R. W. Prager, A. H. Gee and L. Berman. Correction of probe pressure artifacts in freehand 3D ultrasound. To appear in *Medical Image Computing and Computer Assisted Intervention — MICCAI'01*, Utrecht, The Netherlands, October 2001.

G. M. Treece, R. W. Prager, A. H. Gee and L. Berman. Volume measurement of large organs with 3D ultrasound. In *Proceedings of Medical Image Understanding and Analysis*, pages 133-136, London, UK, July 2000.

G. M. Treece, R. W. Prager, A. H. Gee and L. Berman. Volume measurement of large organs with 3D ultrasound. In *Proceedings of SPIE Vol. 3982, Medical Imaging 2000 (Ultrasonic Imaging and Signal Processing)*, pages 2-13, San Diego, California, February 2000.

A. Gee, R. Prager and L. Berman. Non-planar reslicing for freehand 3D ultrasound. In *Medical Image Computing and Computer-Assisted Intervention — MICCAI'99*, pages 716-725, Cambridge UK, September 1999 (LNCS 1679, Springer).

Bibliography

A. Gee, R. Prager and L. Berman. Non-planar reslicing for freehand 3D ultrasound. In *Proceedings of Medical Image Understanding and Analysis*, pages 13–16, Oxford, UK, 1999.

G. Treece, R. Prager, A. Gee and L. Berman. Surface interpolation from sparse cross-sections using region correspondence. In *Proceedings of Medical Image Understanding and Analysis*, pages 17–20, Oxford, UK, 1999.

R. Prager, A. Gee, M. Pearson and L. Berman. Practical segmentation of 3D ultrasound. In *Proceedings of Medical Image Understanding and Analysis*, pages 161–164, Oxford, UK, 1999.

G. Treece, R. Prager, A. Gee and L. Berman. Volume measurement in sequential freehand 3-D ultrasound. In *Proceedings of the 16th International Conference on Information Processing in Medical Imaging*, pages 70–83, Visegrád, Hungary, June 1999 (LNCS 1613, Springer).

R. Prager, A. Gee and L. Berman. Real-time tools for freehand 3D ultrasound. In *Medical Image Computing and Computer-Assisted Intervention — MICCAI'98*, pages 1016–1023, Cambridge MA, October 1998 (LNCS 1496, Springer).

R. Prager, A. Gee and L. Berman. 3D ultrasound without voxels. In *Proceedings of Medical Image Understanding and Analysis*, pages 93–96, Leeds, July 1998.

Other publications by the Cambridge University 3D Ultrasound Group include:

R. W. Prager, A. H. Gee, G. M. Treece and L. Berman. Decompression and speckle detection for ultrasound images using a homodyned k-distribution. To appear in *Pattern Recognition Letters*.

G. M. Treece, R. W. Prager and A. H. Gee. Volume-based three-dimensional metamorphosis using region correspondence. To appear in *The Visual Computer*.

R. N. Rohling, A. H. Gee and L. Berman. A comparison of freehand 3D ultrasound reconstruction techniques. *Medical Image Analysis*, 3(4):339-359, 1999.

B. V. Levienaise-Obadia and A. H. Gee. Adaptive segmentation of ultrasound images. *Image and Vision Computing*, 17(8):583–588, June 1999.

R. N. Rohling, A. H. Gee and L. Berman. Automatic registration of 3-D ultrasound images. *Ultrasound in Medicine and Biology*, 24(6):841–854, July 1998.

R. N. Rohling, A. H. Gee and L. Berman. Three-dimensional spatial compounding of ultrasound images. *Medical Image Analysis*, 1(3):177–193, April 1997.

Bibliography

R. W. Prager, A. H. Gee and L. Berman. Freehand 3D ultrasound without a position sensor. In *Proceedings of Medical Image Understanding and Analysis*, pages 19-22, London, UK, July 2000.

J. C. Carr, M. M. Fynes, A. H. Gee, R. W. Prager, G. M. Treece, C. Overton and L. Berman. Design of a clinical freehand 3D ultrasound system. In *Proceedings of Medical Image Understanding and Analysis*, pages 15-18, London, UK, July 2000.

J. C. Carr, J. L. Stallkamp, M. M. Fynes, A. H. Gee, R. W. Prager, G. M. Treece, C. Overton and L. Berman. Design of a clinical free-hand 3D ultrasound system. In *Proceedings of SPIE Vol. 3982, Medical Imaging 2000 (Ultrasonic Imaging and Signal Processing)*, pages 14-25, San Diego, California, February 2000.

R. Rohling, A. Gee, L. Berman and G. Treece. Radial basis function interpolation for 3D freehand ultrasound. In *Proceedings of the 16th International Conference on Information Processing in Medical Imaging*, pages 478–483, Visegrád, Hungary, June 1999 (LNCS 1613, Springer).

C. Sherratt, A. Basman, R. Prager and A. Gee. Interactive segmentation of ultrasound images by creep-and-merge. In *Proceedings of Medical Image Understanding and Analysis*, pages 133–136, Leeds, July 1998.

J. C. Carr, A. H. Gee, R. W. Prager and K. J. Dalton. Quantitative visualisation of surfaces from volumetric data. In *Proceedings of the Sixth International Conference in Central Europe on Computer Graphics and Visualization*, pages 57–64, Plzen, Czech Republic, February 1998.

R. N. Rohling, A. H. Gee and L. Berman. Automatic registration of 3-D ultrasound images. In *Proceedings of the International Conference on Computer Vision*, pages 298–303, Bombay, January 1998.

J. C. Carr, W. R. Fright, A. H. Gee, R. W. Prager and K. J. Dalton. 3D shape reconstruction using volumetric intersection techniques. In *Proceedings of the International Conference on Computer Vision*, pages 1095–1100, Bombay, January 1998.

B. V. Levienaise-Obadia and A. H. Gee. Adaptive segmentation of ultrasound images. In *Proceedings of the 1997 British Machine Vision Conference*, volume 1, pages 202–211, Colchester, September 1997.

R. N. Rohling, A. H. Gee, R. W. Prager and L. Berman. 3D spatial compounding of ultrasound images. In *Proceedings of Medical Image Understanding and Analysis*, pages 37–40, Oxford, July 1997.

Bibliography

C. R. Dance, M. H. Syn, R. W. Prager, A. H. Gee, J. P. M. Gosling and L. H. Berman. Interactive segmentation of 3D ultrasound using deformable solid models and active contours. In *Proceedings of Medical Image Understanding and Analysis*, pages 25–28, Oxford, July 1997.

R. N. Rohling, A. H. Gee and L. Berman. Spatial compounding of 3-D ultrasound images. In *Proceedings of the 15th International Conference on Information Processing in Medical Imaging*, pages 519–524, Poultney, Vermont, June 1997 (LNCS 1230, Springer).

R. N. Rohling and A. H. Gee. Correcting motion-induced registration errors in 3-D ultrasound images. In *Proceedings of the 1996 British Machine Vision Conference*, volume 2, pages 645–654, Edinburgh, September 1996.

Versions of some of these papers are available as technical reports from our web server at http://svr-www.eng.cam.ac.uk/.

G. M. Treece, R. W. Prager, A. H. Gee and L. Berman. Correction of probe pressure artifacts in freehand 3D ultrasound — initial results. Technical report CUED/F-INFENG/TR 411, Cambridge University Department of Engineering, April 2001.

R. W. Prager, A. H. Gee, G. M. Treece and L. Berman. Decompression and speckle detection for ultrasound images using a homodyned k-distribution. Technical report CUED/F-INFENG/TR 397, Cambridge University Department of Engineering, November 2000.

A. H. Gee, R. W. Prager, G. M. Treece and L. Berman. Narrow-band volume rendering for freehand 3D ultrasound. Technical report CUED/F-INFENG/TR 392, Cambridge University Department of Engineering, September 2000.

G. M. Treece, R. W. Prager and A. H. Gee. Volume-based three-dimensional metamorphosis using region correspondence. Technical report CUED/F-INFENG/TR 379, Cambridge University Department of Engineering, April 2000.

G. M. Treece, R. W. Prager, A. H. Gee and L. Berman. 3D ultrasound examination of large organs. Technical report CUED/F-INFENG/TR 367, Cambridge University Department of Engineering, December 1999.

P. M. Tuomola, A. H. Gee, R. W. Prager and L. Berman. Body-centered visualisation for freehand 3D ultrasound. Technical report CUED/F-INFENG/TR 362, Cambridge University Department of Engineering, October 1999.

G. M. Treece, R. W. Prager, A. H. Gee and L. Berman. Surface interpolation from sparse cross-sections using region correspondence. Technical report CUED/F-INFENG/TR 342, Cambridge University Department of Engineering, March 1999.

Bibliography

A. H. Gee, R. W. Prager and L. Berman. Non-planar reslicing for freehand 3D ultrasound. Technical report CUED/F-INFENG/TR 340, Cambridge University Department of Engineering, January 1999.

G. M. Treece, R. W. Prager and A. H. Gee. Regularised marching tetrahedra: improved iso-surface extraction. Technical report CUED/F-INFENG/TR 333, Cambridge University Department of Engineering, September 1998.

R. N. Rohling, A. H. Gee and L. Berman. Radial basis function interpolation for 3-D ultrasound. Technical report CUED/F-INFENG/TR 327, Cambridge University Department of Engineering, July 1998.

G. M. Treece, R. W. Prager, A. H. Gee and L. Berman. Fast surface and volume estimation from non-parallel cross-sections, for freehand 3-D ultrasound. Technical report CUED/F-INFENG/TR 326, Cambridge University Department of Engineering, July 1998.

R. W. Prager, A. H. Gee and L. Berman. Stradx: real-time acquisition and visualisation of freehand 3D ultrasound. Technical report CUED/F-INFENG/TR 319, Cambridge University Department of Engineering, April 1998.

R. W. Prager, R. N. Rohling, A. H. Gee and L. Berman. Automatic calibration for 3-D free-hand ultrasound. Technical report CUED/F-INFENG/TR 303, Cambridge University Department of Engineering, September 1997.

R. N. Rohling, A. H. Gee and L. Berman. Automatic registration of 3-D ultrasound images. Technical report CUED/F-INFENG/TR 290, Cambridge University Department of Engineering, May 1997.

R. N. Rohling and A. H. Gee. Spatial compounding of 3-D ultrasound images. Technical report CUED/F-INFENG/TR 270, Cambridge University Department of Engineering, October 1996.

R. N. Rohling and A. H. Gee. Issues in 3-D free-hand medical ultrasound imaging. Technical report CUED/F-INFENG/TR 246, Cambridge University Department of Engineering, January 1996.